A review of performance enhancement of PCM based latent heat storage system within the context of materials, thermal stability and compatibility

Zakir Khan [a]*, Zulfiqar Khan [a], Abdul Ghafoor [b]

[a] Bournemouth University, Sustainable Design Research Cluster, Fern Barrow, Talbot Campus, Poole, Dorset BH12 5BB, UK.

E-mail: zkhan@bournemouth.ac.uk

[b] SMME, National University of Sciences and Technology (NUST), NUST Campus H-12, Islamabad, Pakistan.

E-mail: principal@smme.nust.edu.pk

Corresponding Author:

[a]* Bournemouth University, Sustainable Design Research Cluster, Fern Barrow, Talbot Campus, Poole, Dorset BH12 5BB, UK.

E-mail: zkhan2@bournemouth.ac.uk

Tel.: +44 74592490691

Abstract

Phase change materials (PCM) with their high thermal storage density at almost isothermal conditions and their availability at wide range of phase transitions promote an effective mode of storing thermal energy. Literature survey evidently shows that paraffins and salt hydrates provide better thermal performance at competitive cost. This review paper is focused on the classification of various paraffins and salt hydrates. To acquire long term productivity of LHS system, the thermo-physical stability of both paraffins and salt hydrates; and their compatibility with various plastic and metallic container materials play a vital role. Likewise, the lower thermal conductivity of PCMs affects the thermal performance of LHS system. This article reviews the various thermo-physical performance enhancement techniques such as influence of container shape and its orientation, employment of fins and high conductivity additives, multi-PCM approach and PCM encapsulation. The performance enhancement techniques are focused to improve the phase transition rate, thermal conductivity, latent heat storage capacity and thermo-physical stability. This review provides an understanding on how to maximize thermal utilization of PCM. This understanding is underpinned by an analysis of PCM-Container compatibility and geometrical configuration of the container.

Keywords

Thermal energy storage, Latent heat, Phase change materials, Thermal stability, Heat transfer

Table of Contents

1. Introduction

The continuous and expeditious rise in worldwide economic development is followed up by a strong demand of continuous supply of energy. Energy generated from fossil fuel have fulfilled and served human needs for a long era. However, the fossil fuel resources are limited and due to their fluctuating pricings, the availability of uninterrupted supply of energy is highly uncertain. Moreover, the higher use of conventional fossil fuel is responsible for immense damage to environment, due to emission of harmful gases and impurities in air that leads to recent global warming. These serious challenges have motivated engineers and scientists all over the world to develop technologies to utilize sources of renewable energy so as to avert from technologies that cause environmental hazards, high cost for energy generation and avoid establishing new costly power plants.

Thermal energy storage (TES) system is considered a very critical technology, which possess a great adaption to renewable energies. The storage of excess energy that would otherwise be wasted could work as to bridge the gap between energy requirements and generation. Solar thermal energy can be stored during solar peak hours and it can be utilized during off peak hours/night times, using TES system. Likewise, both in cold and hot climates, electricity consumption varies significantly during day and night timings, due to space heating and air conditioning. Therefore, an effective power consumption management can be achieved by using TES system to store the thermal heat or coolness in off peak loads hours and use it during peak loads hours.

The unpredictable and varying nature of renewable energy affects the supply and demand gap of energy, which can be sorted by adopting robust and responsive energy storage technique. However, the speedy energy storage and its reclamation has been a major challenge. TES can be classified into sensible heat storage (SHS), latent heat storage (LHS) and thermo-chemical categories of heat storage systems. SHS is the most commonly exercised method, e.g. water and rock bed are used to store heat in solar heating systems and in air based heating systems, respectively. However, LHS system is considered the most promising technique for storing thermal energy due to their wide range of availability of PCMs, higher thermal storage density and almost isothermal operation of thermal storage/retrieval. Morrison [1] and Ghoneim [2] reported that to store equal amount of thermal energy from a unit collector area, the storage mass for rock (SHS) will be seven times to that of paraffin 116 wax (LHS), five times to that of medicinal paraffin (LHS) and eight times to that of $Na_2SO_4.10H_2O$ (LHS).

Telkes and Raymond were the pioneers to investigate PCMs in 1940s. However, PCMs were ignored until the energy crisis in late 1970s and early 1980s, which motivated scientists to explore the usage of PCMs in

solar heating systems and other applications. Since then, a good amount of research has been carried out to assess the thermal performance of PCMs in LHS system. Research has explored the design fundamentals, transient behaviour, system optimization and various field applications of PCMs in LHS system. Although, LHS system is more promising than SHS but it lacks practical applications due to low thermal conductivity, poor thermo-physical stability, corrosive nature of PCMs towards its container material, phase segregations and subcooling, irregular melting, volume variation during phase transition and higher cost.

The flexibility of PCM to store and retrieve thermal energy at desired time enables it to be employed in broad range of practical applications. A number of comprehensive review articles have been published with a focus on the encapsulation of PCMs; their different types and techniques, encapsulate materials and their utilization in concentrated solar power plants, heat recovery systems, solar thermal heating systems and various passive residential thermal control applications [3-5]. In recent years, a considerable amount of research has been conducted in identification of various novel PCM composites which possess enhanced form-stability, thermal conductivity and thermal storage density [6-8]. Similarly, metal matrix and metal nanoparticle based phase change composites have presented better thermal conductivity than the typical PCMs and thus it indicates a new paradigm for TES systems [9].

This review paper is focused on classification and selection of PCMs for LHS system. A comprehensive review of organic paraffins and inorganic salt hydrates is presented as these groups of PCMs possess high phase change enthalpy, sharp melting point, cost effectiveness and abundant availability. Also, both paraffins and salt hydrates are the most studied and commercially used groups of PCMs. For long term utilization of LHS system, it is essential that the PCMs should possess long term thermo-physical stability and hold a good compatibility with container material. This review article presents the thermo-physical stability of paraffins and salt hydrates; and their compatibility with various plastic and metallic containers. Due to low thermal conductivity of organic and inorganic PCMs, the productivity of LHS system during thermal energy storage and retrieval is highly affected. This article reviews the performance enhancement techniques such as the effect of container configurations, inclusion of extended surfaces and fins, additives for enhancing thermal conductivity, employing multi-PCMs and encapsulation of PCMs. This review will help in selecting reliable PCM and compatible container material, with efficient geometric configurations to achieve maximum thermal utilization of PCM based LHS system.

2. Classification of latent heat storage materials

LHS system uses PCM as thermal energy storage medium. Thermal energy transfer occurs when PCM is melted from solid to liquid or solidified from liquid to solid. During the phase transition of PCM, thermal energy is stored or retrieved. PCM phase transition occurs at nearly constant temperature and unlike sensible storage medium such as water, rocks or masonry; PCM captures 5-14 times more heat per unit volume. Plenty of research is carried out in identifying several groups of suitable PCMs . The selection of PCM for thermal storage system shall possess desirable thermo-physical, chemical, kinetic and economic properties, as summarized in Table 1.

Table 1

Key design properties of PCM for storage purposes.

Thermal	Physical	Chemical	Kinetic	Economic
Appropriate phase transition temperature	Low vapour pressure (<1 bar)	Compatible with container material	High crystallization rate	Cost effective
High latent heat of fusion and specific heat	High density and small volume change	Long term chemical cycling stability	High nucleating rate to avoid supercooling	Abundant
High thermal conductivity	High phase stability	Highly non-flammable, non-toxic and non-explosive		Available

For the past four decades, an extensive research is carried out in identification of various nature of PCMs in a wide range of phase transition temperature and latent heat of fusion including organic materials (e.g. paraffins, fatty acids), inorganic materials (e.g. salt hydrates, metallic) and eutectics (e.g. mixture of organic-organic, inorganic-inorganic and organic-inorganic materials). Each group of PCMs have their own properties, strengths and limitations. Table 2 shows the detail comparison of various groups of PCMs. It is evident from table 2 that paraffins and salt hydrates can provide a better thermal energy storage medium than others.

Paraffins are made up of mixture of alkanes of type C_nH_{2n+2}. They possess almost similar properties and an increase in chain length ensure higher melting point and latent heat of fusion [10, 11]. Paraffins are widely used as thermal energy storage medium due to their good latent heat values (60 - 269 kJ/kg and ≅ 150 MJ/m^3), varied range of phase transition temperature, low vapour pressure, chemical stability and inert to metal containers, no tendency to supercooling and commercially available in reasonable cost. Paraffins are nontoxic

[11, 12]. Table 3 presents the list of thermo-physical properties of paraffins studied by many researchers and commercially manufactured. Besides various favourable properties, paraffins also have some undesirable characteristics which limit applications such as: low thermal conductivity (≅ 0.2 W/mK) and incompatibility with plastic containers [11, 13-15].

Salt hydrates are compounds of inorganic salt and water of general formula $AB.nH_2O$. Solid-liquid transitions of salt hydrates are actually the dehydration and hydration of salt. Salt hydrates are extensively studied and most important group of PCMs, due to their high latent heat of fusion per unit volume (86 - 328 kJ/kg and ≅ 350 MJ/m^3), higher thermal conductivity than paraffins (≅ 0.7 W/mK) and cheaper cost than paraffins [16]. However, during melting of salt hydrates some anhydrous salt or lower hydrates and water formation takes place and due to difference in densities the anhydrous salt (or lower hydrates) settles at the bottom of the container reducing the active volume of heat storage. Salt hydrates also experience supercooling because of their poor nucleating properties. Moreover, some salt hydrates are corrosive towards container materials [15, 17]. Table 4 presents the thermo-physical properties of salt hydrates found in literature and some of the manufacturing companies.

Table 2

Comparison of various PCM groups.

Classification	**Ref.**	**Organic Materials**		**Inorganic Materials**		**Eutectics** [b]
		Paraffins	Fatty Acids	Salt Hydrates	Metallic [a]	
Formula	[11, 14]	C_nH_{2n+2} (n=12-50)	$CH_3(CH_2)_{2n}.COOH$	$AB.nH_2O$	-	-
Melting Point	[11, 13]	-12-135 ^oC	-7-187 ^oC	-33-120 ^oC	29.8 - 125 ^oC	-30.6 - 93 ^oC
Latent Heat	[11, 13, 14]	60 - 269 kJ/kg	125 - 250 kJ/kg	86 - 328 kJ/kg	25 - 90.9 kJ/kg	100 - 267 kJ/kg
Thermal Conductivity	[13, 15]	0.2 W/m K	0.2 W/m K	0.7 W/m K	40.6 W/m K	0.680 W/m K
Density (kg/m3)	[11-14]	760 (liquid), 900 (Solid)	878 (liquid), 1004 (solid)	1937 (liquid), 2180 (solid)	5910 (solid)	1530 (liquid), 1640 (solid)
Key Features		1. Increase in chain length	1. Unlike paraffins, each	1. Alloys of water and	1. Due to larger weight,	1. No phase segregation during

	results in increased melting point and latent heat. 2. Most commercially used PCMs.	material possesses its own properties. 2. Variation in latent heat and melts over a wide range.	inorganic salts. 2. Greater phase change enthalpy. 3. Most studied group of PCMs	it is not seriously considered.	phase transition. 2. Mixture of two or many organic or inorganic or both components.
Advantages	1. Chemically stable, safe, reliable and non-corrosive. 2. No tendency to supercooling or segregation. 3. Good latent heat of fusion. 4. Compatible with all metal containers. 5. Less expensive and available.	1. High latent heat of fusion. 2. Sharp phase transformation. 3. Fatty acids show reproducible melting and freezing. 4. No supercooling.	1. High latent heat of fusion per unit volume. 2. High thermal conductivity. 3. Small volume change than others. 4. Higher density. 5. Sharp melting point. 6. Available and cheap.	1. High thermal conductivity. 2. Low vapour pressure. 3. High heat of fusion per unit volume.	1. Good thermal conductivity. 2. High latent heat of fusion per unit volume.
Disadvantages	1. Low thermal conductivity and density. 2. Incompatible with plastic container. 3. High volume change, volatile and inflammable.	1. Low thermal conductivity. 2. Low flash point. 3. Instable at high temperature and highly inflammable. 4. Toxic and mild	1. Corrosion on metal containers. 2. Phase segregation. 3. Supercooling. 4. Lack of thermal stability. 5. Slightly toxic	1. Low specific heat capacity. 2. Low heat of fusion per unit weight. 3. Costly	1. Low latent heat of fusion per unit weight. 2. Very costly.

	4. No well-defined sharp melting point.	corrosive. 5. 2-3 times expensive than paraffins.	
Method for improvement	1. Installation of Fins in storage unit. 2. Adding highly thermal conductive additives. 3. Adding fire-retardants	1. Fire retardant additives. 2. Thermal conductivity enhancement additives.	1. Nucleating and thickening agent additives. 2. Mechanical Stirring. 3. Use of excess water. 4. PCM encapsulation.

[a] In metallic category, only potential low melting point PCMs are considered.

[b] In eutectic category, paraffin eutectics, fatty acid eutectics, salt hydrates eutectics, metallic eutectics, salt hydrates– metallic, paraffin– salt hydrates and paraffin– metallic eutectics are considered.

Table 3

Thermo-physical properties of Paraffins

Type of PCM	Ref.	Melting Point (^oC)	Latent Heat of Fusion (kJ/kg)	Specific heat Capacity C_p (kJ/kg K)		Thermal Conductivity (kJ/kg K)		Density (kg/m^3)		Thermal Cycles
				Solid	Liquid	Solid	Liquid	Solid	Liquid	
Dodecane	[15]	−9.6	216				2.21			
RT-9 HC	[18]	-9	260	2		0.2	0.2	880	770	
RT 0	[18]	-1	225	2		0.2	0.2	880	770	
RT 3 HC	[18]	3	200	2		0.2	0.2	880	770	
n-Tetradecane	[12]	6	230							
	[15]	5.8-5.9	258-227			0.21				
RT 8 HC	[18]	8	200	2		0.2	0.2	880	770	
RT 10	[18]	10	190	2		0.2	0.2	880	770	
Paraffin C15	[11]	10	205							
n-Pentadecane	[15]	10	193.9						770	
Paraffin C_{16}	[11]	16.7	237.1							
RT 18 HC	[18]	18	250	2		0.2	0.2	880	770	
n-Heptadecane (C_{17} H_{36})	[19]	18.4	84.7							3000
	[12]	19	240			0.21			760	
Paraffin C_{17}	[11]	21.7	213							
Paraffin C_{16}–C_{18}	[12, 20, 21]	20-22	152							
Paraffin C_{13}–C_{24}	[12, 20]	22-24	189				0.21	900	760	
RT 25 HC	[18]	22-26	230	2		0.2	0.2	880	770	
n-Octadecane	[22, 23]	27.7	243.5	2.14	2.66	0.19	0.148	865	785	
RT 28 HC	[18]	27-29	245	2		0.2	0.2	880	770	
Paraffin C_{18}	[11, 12, 20]	28	244			0.15	0.148	814	774	
n-Octadecane	[15]	28	245			0.358	0.148	814	779	

RT 28 HC	[18]	28	245	2		0.2	0.2	880	770	
Paraffin C_{19}	[11]	32	222							
Paraffin wax	[21, 24]	32	251	1.92	3.26	0.514	0.224	830		
RT 35 HC	[18]	35	240	2		0.2	0.2	880	770	
Paraffin C_{20}	[11]	36.7	246							
			155.5-							
Heneicosane	[15]	40	213					778		
Heptadecanone	[11]	41	201							
Paraffin C_{16}–C_{28}	[12]	42-44	189			0.21		910	765	
RT 44 HC	[18]	44	255	2		0.2	0.2	880	770	
			196.5-							
Docosane	[15]	44	252							
Paraffin (70 wt%) +										
Polypropylene (30 wt%)	[25]	44.77	136.16							3000
	[2, 21,									
P116-Wax	22]	46.7	209	2.89	2.89	0.14	0.277	786		
Paraffin ($C_{22.2}$ $H_{44.1}$) (TG)	[26]	47.1	166							900
3-Heptadecanone	[11]	48	218							
Paraffin C_{20} – C_{33}	[12, 20]	48-50	189			0.21		912	769	
9-Heptadecanone	[11]	51	213							
Paraffin wax 53 (CG)	[26, 27]	53	184			2.05				1500
Paraffin wax 54 (CG)	[28]	53.32	184.48							1500
RT 55	[19]	55	172	2		0.2	0.2	880	770	
Paraffin C_{26}	[11]	56.3	256							
Paraffin ($C_{23.2}$ $H_{48.4}$) (TG)	[26]	57.1	220							900
Paraffin wax 60-62	[28]	57.78	129.7							600
Paraffin wax 58-60	[28]	58.27	129.8							600
Paraffin C_{22} – C_{45}	[12, 20]	58-60	189			0.21		920	795	
RT 64 HC	[18]	64	230	2		0.2	0.2	880	780	
Paraffin wax	[17]	64	173.6			0.346	0.167	916	790	

Paraffin $C_{21} – C_{50}$	[20]	66-68	189		0.21		930	830
RT 70 HC	[18]	69-71	260	2	0.2	0.2	880	770
Paraffin C_{33}	[11]	73.9	268					
Paraffin C_{311}	[11]	75.9	269					
Paraffin natural wax 811	[15]	82-86	85		0.72			
Paraffin natural wax 106	[15]	101-108	80		0.65			
Polyethylene	[12]	110-135	200				9110	870

Table 4

Thermo-physical properties of Salt Hydrates

Type of PCM	Ref.	Melting Point (^oC)	Latent Heat of Fusion (kJ/kg)	Thermal Conductivity (kJ/kg K)		Density (kg/m^3)		Thermal Cycles
				Solid	Liquid	Solid	Liquid	
SN 33	[12]	-33	245					
TH 21	[12]	-21	222					
SN 18	[12]	-18	268					
SP -13	[18]	-13	300	0.6				
STLN 10	[12]	-11	271					
SN 06	[12]	-6	284					
SLT 3	[12]	-3	328					
$LiClO_3 \cdot 3H_2O$	[12, 29]	8	253			1720	1530	
$CCl_3F.17H_2O$	[30]	8.5	210					100
$K_2HPO_4 \cdot 6H_2O$	[11]	14	109					
$NaOH_3\ 5H_2O$	[31]	15						5650
Na_2SO_4 1/2NaCl $10H_2O$	[31]	20						5650
$FeBr_3 \cdot 6H_2O$	[11]	21	105					
SP 21 E	[18]	21-23	160	0.6		1500	1400	
$Mn(NO_3) \cdot 6H_2O$	[20, 32]	25.9					1738	
SP 26 E	[18]	25-27	200	0.6		1500	1400	
$CaCl_2 \cdot 12H_2O$	[11]	29.8	174					
TH 29	[15, 32]	29	188	1.09				
Calcium chloride hexahydrate	[29, 33]	29.8	190.8	1.088	0.54	1802	1562	1000
($CaCl_2\ 6H_2O$)	[34]	23.26	125.4					1000
	[31]	27						5650
	[35]	28	86					1000
$LiNO_3 \cdot 3H_2O$	[20, 29, 32]	30	296					
$LiNO_3 \cdot 2H_2O$	[11]	30	296					

SP 31	[18]	31-33	220	0.6		1300	1100	
$Na_2SO_4 \cdot 3H_2O$	[20]	32	251					
Glauber's salt (Na_2SO_4	[36]	32.4	238					320
$10H_2O$)	[20, 31]	32	254	0.554		1485	1458	5650
$Na_2CO_3 \cdot 10H_2O$	[12]	32-36	246.5					
$CaBr_2 \cdot 6H_2O$	[12, 37]	34	115.5				1956	
$LiBr_2 \cdot 2H_2O$	[11]	34	124					
$Na_2HPO_4 \cdot 12H_2O$	[20, 29]	35-44	280	0.514		1522		
$Zn(NO_3)_2 \cdot 6H_2O$	[11, 12, 37]	36	147		0.469	1937	1828	
$FeCl_3 \cdot 6H_2O$	[12]	37	223					
$Mn(NO_3) \cdot 6H_2O$	[11]	37.1	115				1738	
$CoSO_4 \cdot 7H_2O$	[11]	40.7	170					
$KF \cdot 2H_2O$	[11]	42	162					
$MgI_2 \cdot 8H_2O$	[11]	42	133					
$CaI_2 \cdot 6H_2O$	[11]	42	162					
$K_2HPO_4 \cdot 7H_2O$	[11]	45	145					
$Ca(NO_3)_2 \cdot 4H_2O$	[11, 20]	47	153					
$Zn(NO_3)_2 \cdot 4H_2O$	[11, 12]	45-47	110					
STL 47	[12, 20]	47	221	1.34				
$Mg(NO_3) \cdot 2H_2O$	[11]	47	142					
$Fe(NO_3)_2 \cdot 9H_2O$	[11]	47	155					
$Na_2SiO_3 \cdot 4H_2O$	[11]	48	168					
$K_2HPO_4 \cdot 3H_2O$	[11]	48	99					
$Na_2S_2O_3 \cdot 5H_2O$	[12, 15, 20]	48-49	201-210			1750	1670	
$MgSO_4 \cdot 7H_2O$	[12, 20]	48.5	202					
$Ca(NO_3)_2 \cdot 3H_2O$	[11]	51	104					
$FeCl_3 \cdot 2H_2O$	[11]	56	90					
$Ni(NO_3)_2 \cdot 6H_2O$	[11]	57	169					
SP 58	[18]	56-59	250	0.6		1400	1300	
$MnCl_2 \cdot 4H_2O$	[11]	58	151					

$MgCl_2 \cdot 4H_2O$	[11]	58	178					
$Na(CH_3COO) \cdot 3H_2O$	[12, 15, 20]	58	264-267		0.63	1450	1280	
Sodium acetate trihydrate	[38]	58	230					500
($NaCH_3COO.3H_2O$)	[39]	58	252					100
$Fe(NO_3)_2 \cdot 6H_2O$	[11, 20]	60	126					
NaOH	[12, 20]	64.3	227.6			1690		
$Na_3PO_4 \cdot 12H_2O$	[11, 12]	65-69	190					
ClimSel C70	[12, 20]	70-71	194	0.7	0.5	1400	1400	
$Na_2P_2O_7 \cdot 10H_2O$	[12, 20]	70	184					
$LiCH_3COO \cdot 2H_2O$	[11]	70	150					
E 72	[15]	72	140	0.58				
SP 70	[18]	69-73	150	0.6		1500	1300	
$Al(NO_3)_2 \cdot 9H_2O$	[11]	72	155					
$Ba(OH)_2 \cdot 8H_2O$	[20, 29, 37]	78	265-280	1.225	0.653	2070	1937	
E 83	[15]	83	152	0.62				
$Mg(NO_3)_2 \cdot 6H_2O$	[15, 20, 37]	89	162.8	0.611	0.49	1636	1550	
TH 89	[12, 15]	89	149					
SP 90	[18]	88-90	150	0.6		1650		
$KAl(SO_4)_2 \cdot 12H_2O$	[11]	91	184					
$(NH_4)Al(SO_4) \cdot 6H_2O$	[12]	95	269					
Magnesium chloride	[12, 40]	111.5	155.11	0.704	0.694	1569	1450	500
hexahydrate ($MgCl_2$ $6H_2O$)	[41]	110.8	138					1000
E 117	[15]	117	169	0.7				

3. Long term stability of PCMs

Long term useful life of LHS system is limited by poor thermo-physical stability of PCM and corrosion between PCM and its container material. In last two decades, many researchers have indicated the importance of long term stability of PCM-container system [12, 14, 17]. Murat and Khamid [15] suggested that prior to commercial development; the PCMs should be subjected to at least 1000 thermal cycles to examine the long

term stability. In this section, a detail review is carried out on thermal stability and corrosion behaviour of various PCM-container materials.

3.1 Thermo-physical stability of PCM

In this section, the thermal stability of paraffins and salt hydrates has been reviewed.

3.1.1 Paraffins

Sari et al. [19] investigated thermal stability of microencapsulated n-heptadecane for 5000 melt-freeze cycles. Perkin Elmer Diamond DSC (Differential scanning calorimeter) and electric hot plate setup were used as thermal and cycling equipment. They observed good stability of thermo-physical properties of microencapsulated n-heptadecane as the melting point and latent heat of fusion before and after the 5000 thermal cycles varied from 18.4-18.9 ^{o}C and 84.7-94.5 kJ/kg, respectively.

Alkan et al. [25] conducted 3000 thermal cycles of paraffin and polypropylene composite. Setaram DSC 131 and electric hot plate setup were used as thermal and cycling equipment. The results from DSC depicted a small variation in melting point and latent heat of fusion of paraffin within the composite from 44.77-45.52 ^{o}C and 136.16-116.12 kJ/kg, respectively. It was deduced from stability tests that the composite can be used for solar heating applications.

Hadjieva et al. [26] studied variation in thermo-physical properties of three technical grade hydrocarbons $C_{22.2}H_{44.1}$, $C_{23.2}H_{40.4}$ and $C_{24.7}H_{51.3}$. DSC with Mettler TA 3000 system and thermostatic bath setup were used to conduct 900 thermal cycles. $C_{22.2}H_{44.1}$ showed a stable behaviour to thermal cycles with a minor change in melting point and latent heat, from 47.1-46.6 ^{o}C and 166-163 kJ/kg, respectively. Likewise, $C_{23.2}H_{40.4}$ displayed no degradation in the thermo-physical properties after 900 thermal cycles. The change in phase transition temperature and latent heat were negligible, such as from 57.1-57.8 ^{o}C and 220-224 kJ/kg, respectively. Whereas, $C_{24.7}H_{51.3}$ degraded abruptly showing low latent heat capacity and noticeable change in phase transition range. Because of cheap price and highest enthalpy, $C_{23.2}H_{40.4}$ was proposed an efficient material for LHS system.

Shukla et al. [28] evaluated three paraffin waxes of different temperature specified as sample A (m.p 58-60 ^{o}C), sample B (m.p 60-62 ^{o}C) and sample C (m.p 54 ^{o}C). Rheometric scientific ltd. DSC and oven were used to conduct 600 thermal cycles for sample A and B, whereas, sample C was examined for 1500 thermal cycles. DSC results indicated significant degradation in transition temperature and enthalpy of sample A and B.

However, sample C was most stable even after 1500 thermal cycles and was proposed as a good PCM for LHS system.

Sharma et al. [42] examined commercial grade paraffin wax 53. Rheometric scientific ltd. DSC and electric hot plate setup were used to conduct 300 accelerated melt-freeze cycles. Paraffin wax was found to be stable PCM with a small change in latent heat of fusion, from 184-165 kJ/kg. Later on, the same PCM was investigated for 1500 thermal cycles [27]. The results from DSC showed a slight change in melting point (53-50 ^{o}C), whereas, a noticeable change was observed in latent heat (184-136 kJ/kg).

Table 3 provides detail list of paraffins along with their transition temperature, latent heat of fusion, thermal conductivity, density and thermal cycles. The experimental results show that thermo-physical properties of paraffins do not degrade after repeated thermal cycles.

3.1.2 Salt Hydrates

Calcium chloride hexahydrate ($CaCl_2.6H_2O$) is the most studied PCM in salt hydrates group. $CaCl_2.6H_2O$ experiences continuous phase separation and causes either formation of $CaCl_2.4H_2O$ or other hydrates, with repeated thermal cycles, which settle down in the container.

Kimura and Kai [33] examined thermo-physical stability of $CaCl_2.6H_2O$ using Perkin elmer DSC and two tubes heat exchanger for carrying 1000 thermal cycles. They used excess water to control the formation of other hydrates and to increase solubility. NaCl was mixed for its good nucleating potentials. The mixture was tested for 1000 thermal cycles. They noticed a good repeatability of thermo-physical properties and no phase separation.

Fellechenfeld et al. [35] used strontium chloride hexahydrate as nucleating agent and silica gel as thickener in $CaCl_2.6H_2O$. They used Mettler DSC and water bath setup for performing 1000 thermal cycles. They noticed no phase separation and no degradation of thermo-physical properties. Also, Tyagi et al. [34] examined the thermal stability of $CaCl_2.6H_2O$, using TA Instruments DSC Q-100 to perform 1000 accelerated thermal cycles of cooling and heating and observed a small variation in latent heat of fusion but stability in transition temperature.

Marks [36] evaluated the thermal stability of pure Glauber's salt ($Na_2SO_4.10H_2O$) and thickened one. Attapulgite clay was employed as thickener and Borax ($Na_2B_4O_7.10H_2O$) was mixed as nucleating agent. Calorimeter and thermal cycling chamber were used to conduct 320 thermal cycles on both pure and thickened

Glauber's salt. It was deduced from thermal cycles that thermo-physical properties of pure Glauber's salt degrade quicker than thickened mixture. However, it was reported that due to declination in thermal capacity, both pure and thickened Glauber's salt were rejected for long term LHS system.

Porisini [31] evaluated thermal stability of commercial grade salt hydrates specified as sample A ($NaOH.3.5H_2O$), sample B (Na_2SO_4.½$NaCl.10H_2O$), sample C ($CaCl_2.6H_2O$) and sample D ($Na_2SO_4.10H_2O$). He used thermostatic chamber to conduct 5650 thermal cycles on each sample. Sample A and sample B failed after 10 and 300 thermal cycles, respectively. Sample D also experienced declination in thermal properties after 100 thermal cycles. However, sample C showed good thermo-physical stability even after 5650 thermal cycles.

Kimura and Kai [30] investigated thermal stability of Trichlorofluoromethane heptadecahydrate ($CCl_3F.17H_2O$). Polyacrylamide was added as thickener and Tetrabutyl ammonium fluoride hydrate was added as nucleating agent. Perkin elmer DSC and glass beaker with water jacket were used to carry 100 thermal cycles of the mixture. The PCM showed good thermal stability and it was concluded that it can be used for coolness storage.

Wada et al. [38] conducted thermal stability test of three samples of sodium acetate trihydrate specified as guaranteed grade, technical grade and technical grade with added thickener. Polyvinyl alcohol and sodium pyrophosphate decahydrate were added as thickener and nucleating agent. Calorimeter and thermal bath were used to carry 500 thermal cycles on each sample. It was reported that enthalpy capacity of guaranteed grade sample degrade comparatively quicker than technical grade sample. It was also observed that technical grade with thickener sample experienced little declination in thermo-physical properties during thermal test. Kimura and Kai [39] also tested 220g of same sodium acetate trihydrate which was examined by Wada et al [38]. Disodium phosphate was used as nucleating agent and excess water to increase solubility. They prepared four samples of different ratio of water. They observed phase separation for all four samples and no noticeable improvement in stability of hydrate because of excess water. They concluded that due to severe phase separation, this hydrate cannot be considered as a material for LHS system. The conclusion made by Wada et al. [38] and Kimura and Kai [39] comes in contradiction. The reason for phase separation might be because of the small amount of sample (30g) taken by Wada et al. [38] in comparison to Kimura and Kai [39].

Sebaii et al. [40] conducted thermal stability and container material compatibility tests of commercial grade magnesium chloride hexahydrate ($MgCl_2.6H_2O$). Shimadzu DSC- 60 and Heraeus D-6450 electric oven were used to carry out 500 thermal cycles and SEM for compatibility test. It was noticed that $MgCl_2.6H_2O$

experienced phase segregation in unsealed container even with excess water and was not compatible with container material (aluminium or stainless steel). The changes in transition temperature (111.5–124.12 ^{o}C) and latent heat of fusion (155.11-85 kJ/kg) were significant and thus it could not qualify to be used as thermal storage material. Later on, the same researcher investigated thermal stability for 1000 thermal cycles of $MgCl_2.6H_2O$ with sealed container and excess water [41]. It was observed that sealing of container and excess of water improved thermo-physical stability with slight change in transition temperature (110.8-115.39 ^{o}C) and latent heat of fusion (138-130.28 kJ/kg).

Table 4 provides detail list of salt hydrates along with their transition temperature, latent heat of fusion, density and thermal cycles. The experimental results show that salt hydrates need nucleating agents and thickeners to sustain long term thermal stability.

3.2 Container-PCM compatibility

For long term stability of LHS system, the compatibility between selected PCM and its container material is considered very important.

Lazaro et al. [43] evaluated the compatibility of four commercial organic PCMs (C16-C18, RT20, RT25 and RT26) and one inorganic PCM (TH24) against plastic materials (PP, LDPE, HDPE and PET). During ten months of experimental investigations, through visual inspection and gravimetric analysis, moisture sorption and migration of organic PCM in plastic containers were detected. The results depicted that due to highest mass variation in LDPE encapsulation, it was discarded against all PCMs. PET encapsulates material produced good mass stability against C16-C18, RT 20, RT 25 and RT 26. However, PP, PET and LDPE indicated increase in material mass due to moisture sorption during TH 24 molten salt test and therefore only HDPE encapsulate material were recommended.

Cabeza et al. [44] tested the corrosive nature of zinc nitrate hexahydrate ($Zn(NO_3)_2.6H_2O$), sodium hydrogen phosphate dodecahydrate ($Na_2HPO_4.12H_2O$) and calcium chloride hexahydrate ($CaCl_2.\ 6H_2O$) upon short term 14 days contact with metals. They observed that apart from stainless steel (Mat. No.1.4301), $Zn(NO_3)_2.6H_2O$ appeared to be extremely corrosive to brass (Ms58 Flach), steel (Mat. No. 1.0345), aluminium (EN AW-2007) and copper (E-Cu 57). $Na_2HPO_4.12H_2O$ proved to be compatible with brass, copper and stainless steel, whereas, it was found very corrosive against aluminium. $CaCl_2.\ 6H_2O$ was found compatible with brass and copper, while it was very corrosive against aluminium, stainless steel and steel.

Cabeza et al. [45] investigated the corrosive nature of same three salt hydrates, as in [44], upon medium term 75 days contact with metals. They reported that while using $Zn(NO_3)_2.6H_2O$ as thermal energy storage medium only stainless steel should be considered for container material. $Na_2HPO_4.12H_2O$ showed good compatibility with brass and stainless steel. Aluminium indicated aggressive corrosion, whereas, copper and steel corrode at slow rate. $CaCl_2.6H_2O$ was observed to have good compatibility with copper, brass and stainless steel but can corrode steel and aluminium at slow rate.

Cabeza et al. [46] conducted compatibility test of two salt hydrates sodium acetate trihydrate (NaOAc. $3H_2O$) and sodium thiosulfate pentahydrate ($Na_2S_2O_3$. $5H_2O$) with the same five metals as in [44]. It was reported that both salt hydrates showed good compatibility with aluminium, steel and stainless steel, however, both salt hydrates were aggressively corrosive towards brass and copper.

Farrell et al. [47] examined the galvanic coupling of aluminium-copper in contact with sodium sulphate decahydrate and sodium chloride eutectic and sodium acetate with additives. It was observed that aluminium alloy 2024 was corroded by both PCMs. The corrosion was more aggressive when aluminium was in contact with sodium acetate in the presence of copper.

Nagano et al. [48] inspected material compatibility of magnesium nitrate hexahydrate ($Mg(NO_3)_2.6H_2O$) with magnesium chloride hexahydrate ($MgCl_2.6H_2O$) as an additive, and six metals. Each metal sample was placed for 90 days in a glass tube of 60 ml at a constant temperature of 95^oC. It was reported that copper, steel and brass experienced strong corrosion with a 90 days mass loss of 0.11g, 0.0843g and 0.0284g, respectively. Stainless steel SUS 304 and SUS 316 underwent a very small mass loss of 0.00107g and 0.00017g, respectively. However, it can be seen from Fig. 1 that almost all the surface of SUS 304 and a small portion of SUS 316 were covered with dotted red-brown rust. Aluminium was the only metal that was not affected by the salt hydrates mixture.

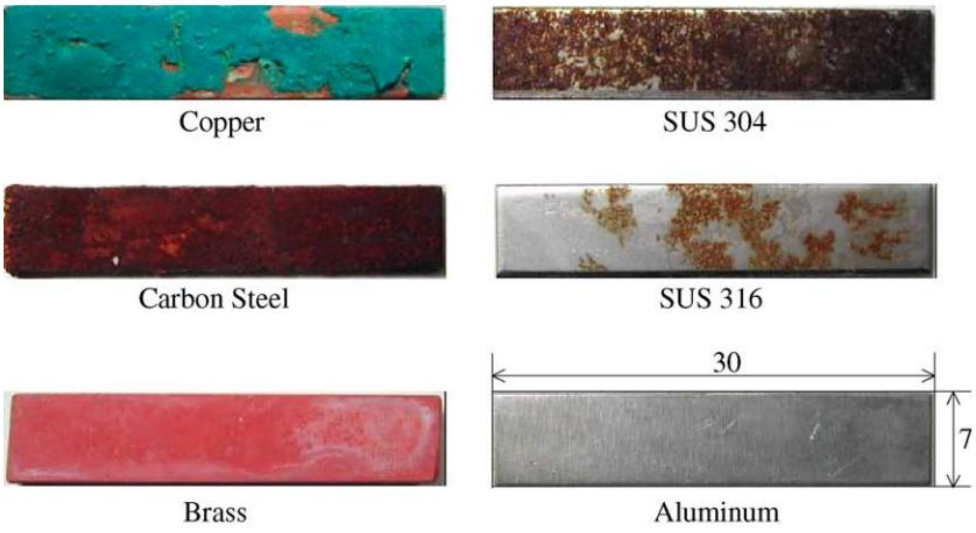

Fig.1. Mg $(NO_3)_2 \cdot 6H_2O$ compatibility test with metals [48].

Garcia et al. [49] studied the corrosion behaviour of commercial grade Glauber's salt (NA_2SO_4. $10H_2O$) with aluminium alloys (Al 1050, 2024, 3003 and 6063). Aluminium alloy specimens were partly and fully immersed in the Glauber's salt for 90 days at 45°C. Al 2024 experienced strong pitting corrosion and degradation of PCM due to formation of Na-Al alkaline carbonates due to the reaction with CO_2 from the air. Al 1050 and 3003 displayed an excellent compatibility with Glauber's salt. Al 6063 also showed good resistance to corrosion when the sample was fully immersed, whereas a loss of brightness and stained surface was notice when it was partially immersed.

Pere et al. [50] presented the corrosion behaviour of two metals and two metal alloys in contact with eleven different salt hydrates used in cooling and heating applications. Each material specimen was examined after week 1, 4 and 12 to examine corrosion rate, salt precipitation and bubbles formation. They reported that commercial PCM S10 can only be used with stainless steel. Similarly, PCM C10 showed good compatibility with both aluminium and stainless steel. $NaOH.1.5H_2O$, $ZnCl_2.3H_2O$ and $K_2HPO_4.6H_2O$ were well suited with stainless steel, whereas $NaOH.1.5H_2O$ could also be used with carbon steel while $ZnCl_2.3H_2O$ and $K_2HPO_4.6H_2O$ could be used with copper. Stainless steel indicated good resistance to corrosion when brought in contact with heating application PCMs. Commercial PCM C48 also showed good compatibility with carbon steel and aluminium. $MgSO_4.7H_2O$ could be used with aluminium and $K_3PO_4.7H_2O$ was suitable to be used with carbon steel.

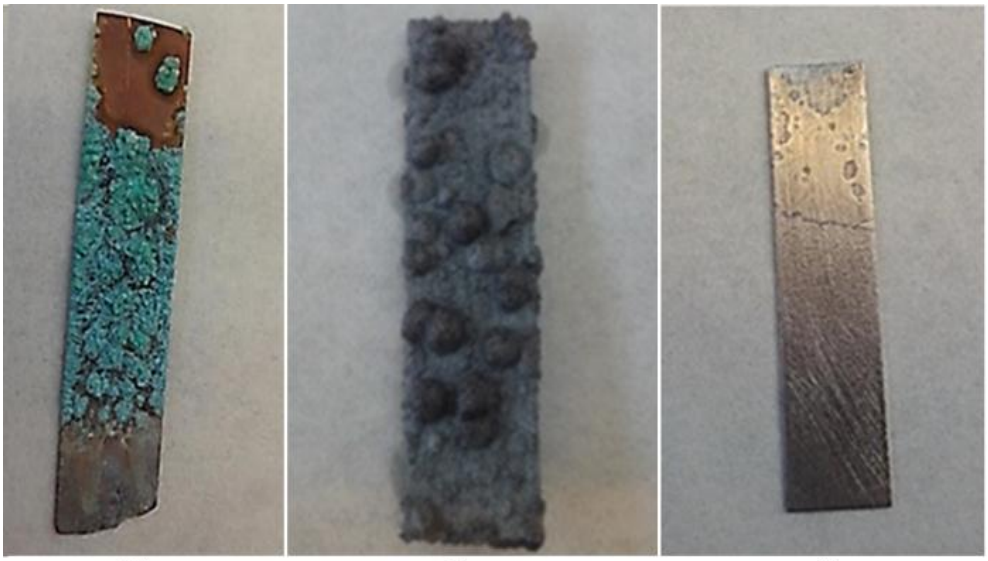

Fig.2. Corrosion tests results: (A) S10 - Copper corrosion test for 12 weeks (B) $ZnCl_2.3H_2O$ - Aluminium corrosion test for 12 weeks, and (C) $Zn(NO_3)_2.4H_2O$-Carbon steel corrosion test for 4 weeks.

Table 5

A list of compatible PCM with container material.

PCM	Ref.	Container Materials				
		Brass	**Copper**	**Aluminium**	**Stainless steel**	**Carbon Steel**
$Zn(NO_3)_2.6H_2O$	[44]	No	No	No	Yes	No
	[45]	No	No	No	Yes	No
$Na_2HPO_4.12H_2O$	[44]	Yes	Yes	No	Yes	No
	[45]	Yes	Caution	No	Yes	Caution
$CaCl_2.6H_2O$	[44]	Yes	Yes	No	Caution	No
	[45]	Yes	Yes	Caution	Yes	Caution
$NaOAc.3H_2O$	[46]	Caution	Caution	Yes	Yes	Yes
$Na_2S_2O_3.5H_2O$	[46]	No	No	Yes	Yes	Yes
$Mg(NO_3)_2 \cdot 6H_2O$	[47]	No	No	Yes	Yes	No
Glauber's salt	[49]			Al 1050 Yes		
($Na_2SO_4.10H_2O$)				Al 2024 No		
				Al 3003 Yes		
				Al 6063 Caution		
S10 (Na_2SO_4 + NH_4Cl + sepiolite)	[50]		No	Caution	Yes	No
C10 (Na_2SO_4 + H_2O + additives)	[50]		No	Yes	Yes	No
$ZnCl_2.3H_2O$	[50]		Yes	No	Yes	No
$NaOH.1.5H_2O$	[50]		No	No	Yes	Caution
$K_2HPO_4.6H_2O$	[50]		Caution	No	Yes	No
S46 ($Na_2S2O_3.5H_2O$ +sepiolite+	[50]		No	Caution	Yes	No
fumed silica)						
C48 (CH_3OONa+H_2O+ additives)	[50]		No	Yes	Yes	Yes
$MgSO_4.7H_2O$	[50]		No	Yes	Yes	No
$Zn(NO_3)_2.4H_2O$	[50]		No	No	Yes	No
$K_3PO_4.7H_2O$	[50]		No	No	Yes	Yes
$Na_2S_2O_3.5H_2O$	[50]		No	Caution	Yes	Caution

Table 5 represents the experimental work carried out in identification of container-PCM compatibility. It is observed from literature that paraffins have poor compatibility with plastic containers; however, high density polyethylene (HDPE) has exhibited good compatibility with paraffins. Similarly, majority of inorganic salt hydrates have corrosive nature with metal containers; however, stainless steel has exhibited good compatibility.

4. LHS system performance analysis and enhancement

LHS system with its high thermal storage density at nearly isothermal process provides a better choice of heat storage. However, due to low thermal conductivity and poor thermo-physical stability of PCMs, the LHS system productivity during charging and discharging processes are highly affected. As a result, large scale practical utilization of LHS system remains inefficient. Therefore, it is necessary to enhance the shortcomings of the LHS system by adopting various performance enhancement techniques. In recent years, few review papers are published on thermal performance enhancement of LHS system [51-53]. These review papers have highlighted the improvement in thermal conductivity of PCMs by using nanostructures, techniques to enhance the thermal performance of PCMs in concentrated solar power plants and the effect of inlet and outlet temperature, and mass flow rate of heat transfer fluid (HTF) on thermal performance of PCM. However, this section reviews the most recent developments in geometrical orientations of containers to enhance heat flow in order to boost the phase transition rate, thermal conductivity enhancement of PCMs by extended surfaces and additives, improvement in thermal storage capacity by multi PCM, and encapsulation of PCMs to ensure better thermal conductivity and thermo-physical stability. This section is focused on techniques that influence the phase transition rate, thermal conductivity, latent heat storage capacity and thermo-physical stability of PCMs.

4.1 PCM container configuration

After the selection of PCM, the geometry of PCM container plays an important role in thermal performance of LHS system. The PCM container geometric configuration has a direct impact on the heat transfer nature and ultimately affects the phase transition rate. PCM containers are of typically rectangular, concentric annular tube, spherical and shell and tube configurations. The most studied geometric configuration is shell and tube, for the fact that it has minimal heat loss characteristic and substantial utilization in engineering applications.

During melting process, heat is transferred from hot surface to PCM through conduction and as the heat transfer continues, the amount of melted PCM increases near hot surface and thus natural convection takes over.

Lamberg at al. [54] simulated the melting time of PCM in rectangular container of 96mm height, 20mm thickness and 41mm depth; with and without natural convection. It was justified by comparison with experimental results that LHS system with natural convection took almost half melting time to that without convection consideration. Kamkari et al. [55] studied the dynamic thermal performance of lauric acid as PCM in rectangular container at different inclination angles of 0^o, 45^o and 90^o. The container hot wall was isothermally heated whereas the other walls were thermally insulated. Various experiments were conducted for hot wall temperatures of 55 ^{o}C, 60 ^{o}C and 70 ^{o}C. It was reported that hot wall positioning in rectangular container played a vital role in formation of natural convection currents and therefore affecting the heat transfer rate and melting rate. Initially, the heat transfer in vertical hot wall container was dominated by conduction as temperature contours were almost parallel to hot wall. The viscous forces were overcome by buoyant forces as the temperature of liquid PCM increased, and eventually the hot liquid PCM climbed along the vertical hot wall. The heat transfer was dominated by natural convection and therefore it increased the melting rate in upper portion of solid-liquid interface by increasing local heat transfer due to hot liquid PCM. The temperature of liquid PCM decreased as it descended along the solid-liquid interface and therefore the heat transfer at lower portion of container was found lesser than upper portion. Also, the accumulated hot liquid PCM at upper portion of container absorbed a considerable amount of heat from hot wall and resulted in stratified liquid layer. In case of 45^o inclination of hot wall, contrary to vertical hot wall observations, the stratified temperature layers did not appear at the upper portion of container which means that heat transferred from liquid to solid PCM and thus it increased the melting rate. In case of horizontal hot wall, the uniform temperature distribution along the solid-liquid interface resulted in uniform melting rate. The heat transfer enhancement ratio for horizontal hot wall container was found twice to that of vertical hot wall container, as shown in Fig. 3.

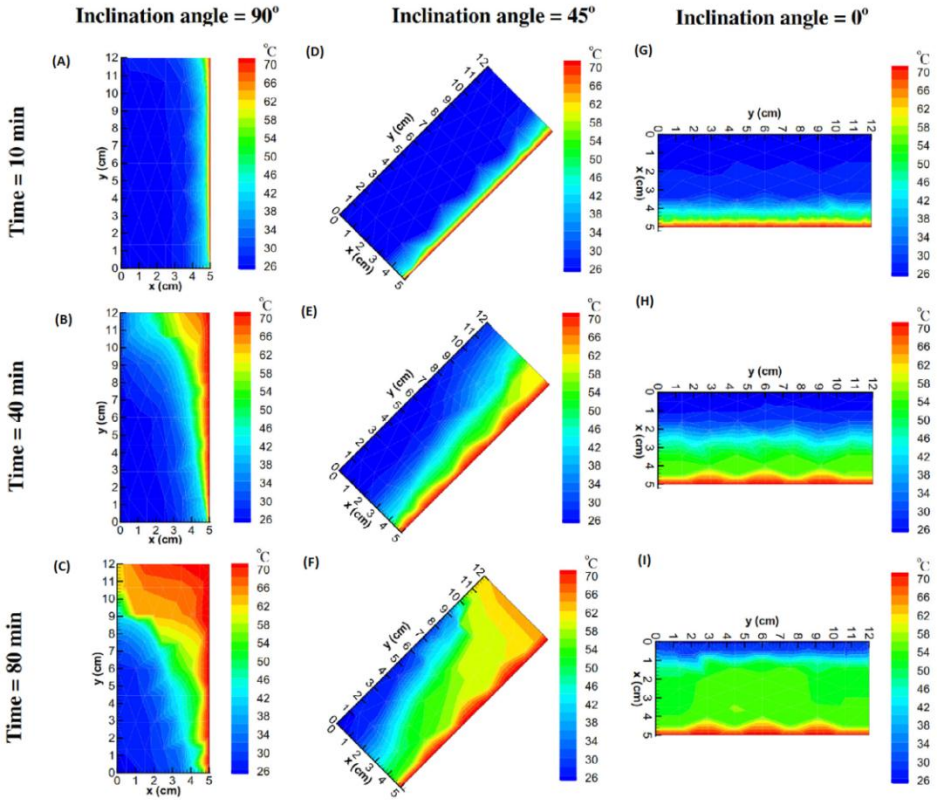

Fig.3. Temperature contours of rectangular container with different inclination angles when hot wall is at 70 ^{o}C [55].

Constrained and unconstrained melting of n-Octadecane in a sphere container is experimentally examined by Tan [56]. In constrained melting case, solid PCM is attached to thermocouple to prevent it from sinking to the bottom of sphere due to gravity. It was reported that in unconstrained melting case, the start of PCM melt was dominated by heat conduction across the sphere wall. As the PCM melted then due to difference in densities the solid PCM sank to the bottom. Therefore, the lower portion of solid PCM was melted by heat conduction from inner wall and the upper portion was melted by natural convection caused due to buoyancy effect. In constrained melting case, conduction heat was responsible for initial inward concentric melting and later the melting was dominated by natural convection, making an oval shape at the top half of solid PCM. The upper half of the solid PCM was melting at higher rate than the bottom half. Natural convection cells were formed at bottom half and it caused waviness profile at bottom of solid PCM.

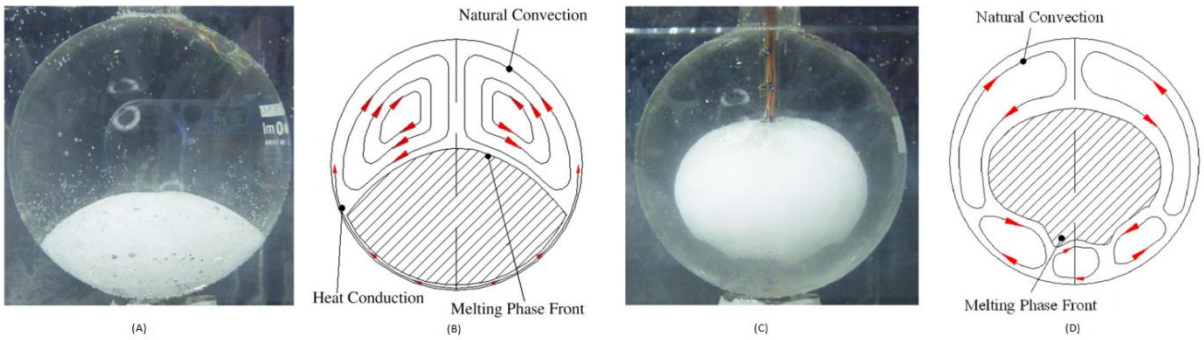

Fig.4. (a) Unconstrained melting inside sphere, (b) Representation of heat conduction and natural convection in unconstrained melting, (c) Constrained melting inside sphere and (d) Representation of natural convection in constrained melting [56].

The melting behaviour of n-eicosane in cylindrical container was studied by Jones et al. [57]. The experimental examination was focused on solid-liquid interface, temperature measurements and volumetric liquid fraction. Digital image processing technique was used to locate the melt front in cylindrical container. It was reported that melting process was dominated by four different regimes, such as (a) pure conduction, (b) conduction and natural convection, (c) natural convection and (d) solid shrinkage. As shown in Fig. 5(a), the melt front was found thin and parallel to vertical hot boundaries of cylindrical container, it depicted that initially melting was dominated by conduction. It was noticed that as the melting increased, the melt front thickness along vertical direction varied, with maximum molten layer thickness was observed at top of container. It indicated the buoyant forces driven natural convection began to strengthen and moving the hot molten layer to top of container. However, the melt front was still almost uniform to vertical hot walls and it was suggested that this regime could be a mixed conduction and natural convection, as shown in Fig. 5(b). Later, the melting was found more influenced by natural convection and the molten layer thickness varied along the vertical hot walls, as shown in Fig. 5(c). Lastly, the top portion of PCM was completely melted by convection and this regime was called shrinking solid, as shown in Fig. 5(d). Similarly, Shmueli et al. [58] numerically investigated the melting behaviour of PCM in vertical cylindrical container, isothermally heated from sides, insulted at bottom and top portion of container was bare to air. The melting behaviour was found similar to that of Jones et al. [57].

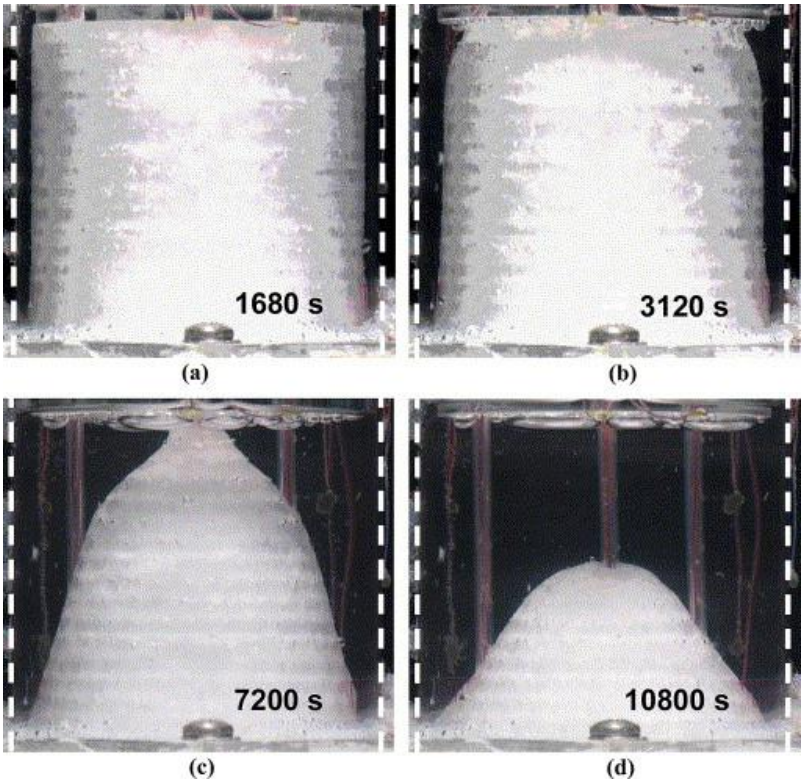

371

372 **Fig.5.** Melting nature of wax in cylindrical container with wall temperature of 45 ^{o}C at various time intervals

373 such as; (a) 1680 seconds, (b) 3120 seconds, (c) 7200 seconds and (d) 10800 seconds [57].

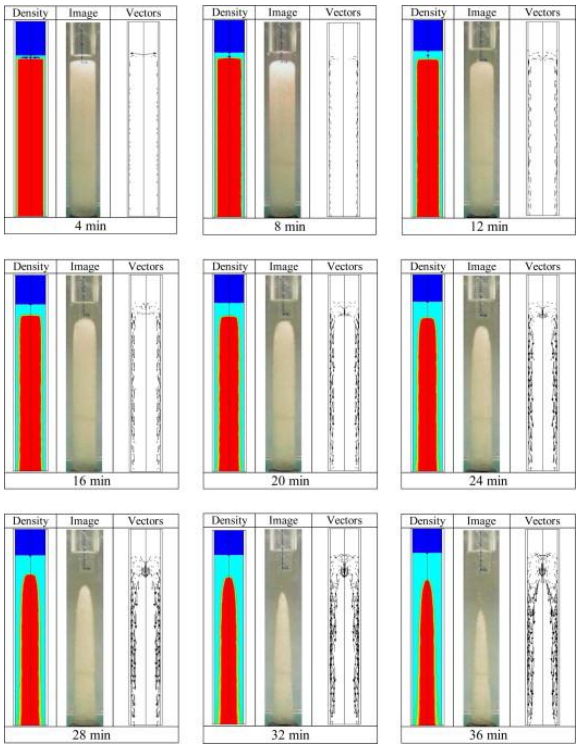

374

375 **Fig.6.** Comparison of simulate density and vector maps with experimental images [58].

Theoretical optimization of two different models of cylindrical containers is carried out by Esen et al. [21]. In the cylindrical model, the PCM was stored in pipe and HTF was flowing parallel in cylindrical portion. Whereas in pipe model, the PCM was stored in cylindrical side and HTF was flowing in pipe. A series of numerical tests were carried out to investigate the effect of different PCMs, radii of cylinder and pipe, mass flow rate and inlet temperature of HTF on melting time. It was concluded from the results that pipe model required less time than cylindrical model to melt the PCM, due to the fact that thicker mass of PCM takes longer time to melt and less amount of heat loss from the HTF to surrounding.

Esapour et al. [59] investigated the melting behaviour of RT35 in various arrangements of shell and multi-tubes. As exhibited in Fig. 7, RT35 was stored in middle tube/shell, whereas HTF was made to flow in inner tubes and outer one .The effect of number of inner-tubes on charging process was analysed. It was reported that an increase in inner-tubes from 1 to 4 enlarged the molten region and therefore the regime was dominated by convection heat transfer, which led to enhanced melting rate. According to Fig. 8, in case A, both the heating surfaces (inner tube and outer tube) were installed wide apart which resulted in weak natural convection effects and thus the melting rate was slow. Whereas in case B, C and D, heat transfer surface was increased by distributing thinner tubes across the shell. The buoyant force increased as the vortices merged to form a large vortex and therefore the melting rate was accelerated. The utilization of 4 inner-tubes in shell reduced the melting time by 29% to that of single inner-tube.

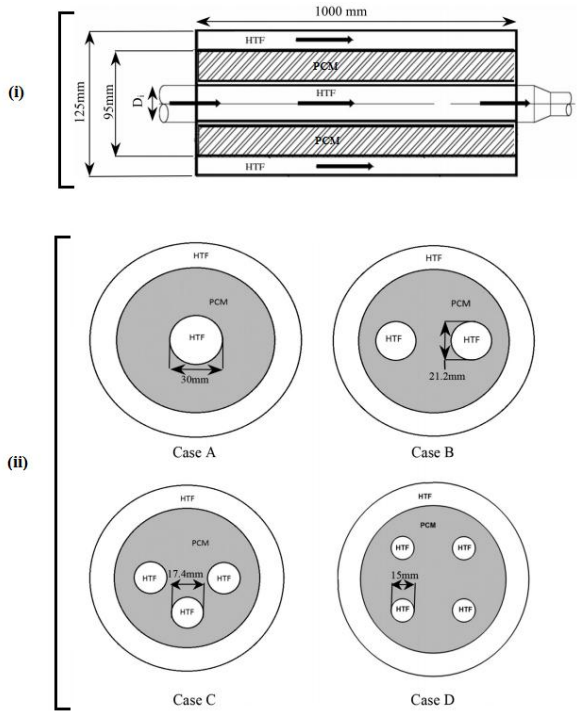

Fig.7. (i) Schematic of physical model of multi-tube configuration, (ii) Configuration of multi-tube cases [59].

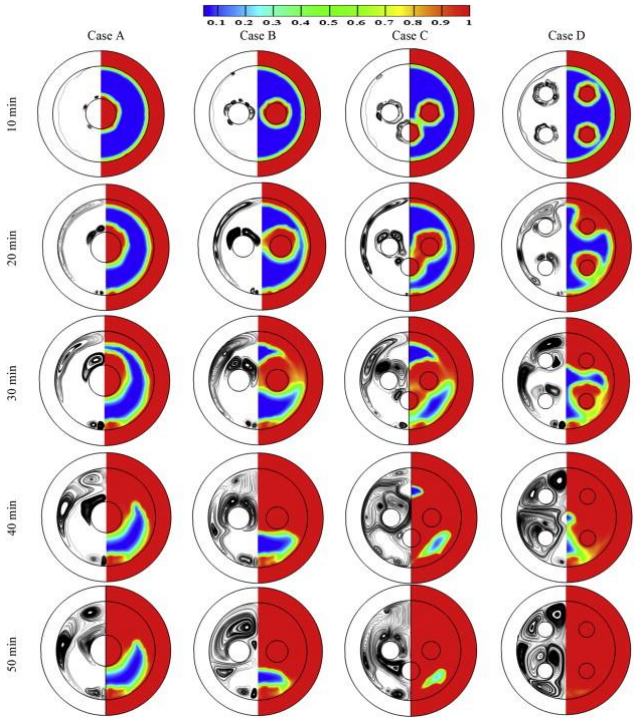

Fig.8. Liquid fraction contours for various multi-tube arrangements [59].

Vyshak and Jilani [60] conducted a comparative study on total melting time of PCM stored in rectangular, cylindrical and cylindrical shell containers of same volume and heat transfer surface area. The investigation was carried out for various values of PCM mass and inlet temperature of HTF. It was deduced that cylindrical shell configuration took least time to store the same amount of thermal energy as compared to other two configurations. It was also reported that with increase in mass of PCM, the cylindrical shell performance was more pronounced, comparatively. The results showed that melting time for rectangular container was nearly half to that of cylindrical container. Zivkovic and Fujii [61] also reported the similar results for rectangular and cylindrical configuration.

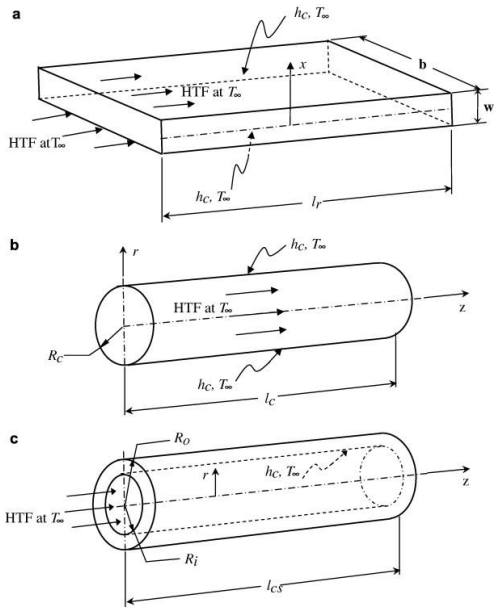

405

406 **Fig.9.** Comparison of various container models: (a) Rectangular container model, (b) cylindrical container
407 model and (c) cylindrical shell container model [60].

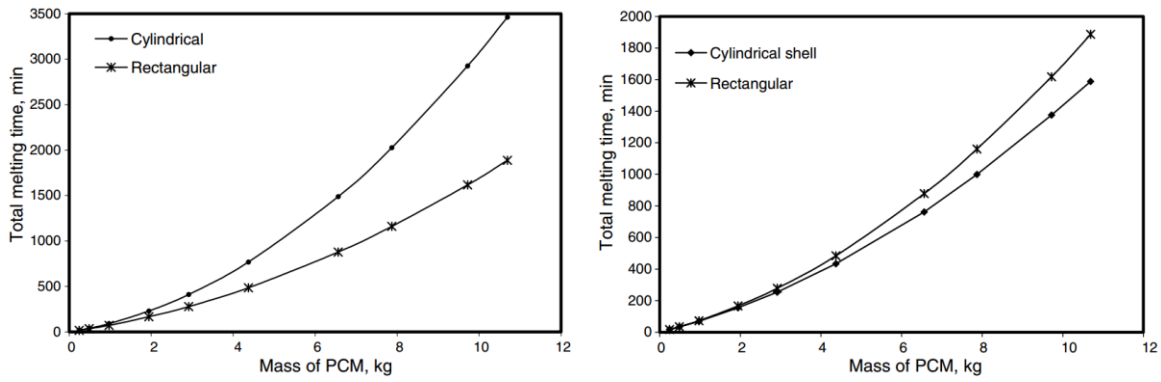

408

409 **Fig.10.** Comparison of total melting time vs mass of PCM for cylindrical and rectangular containers and
410 cylindrical shell and rectangular containers [60]

411 In case of solidification process, the heat transfer is dominated and influenced by conduction. Therefore,
412 the container orientation has insignificant influence on solidification rate. Seddegh et al.[62] numerically
413 evaluated the thermal behaviour of Paraffin wax in horizontal and vertical orientations of shell and tube
414 container. During melting process, it was noticed that the heat transfer in horizontal system was more effective
415 in melting the upper half of PCM than the lower half, whereas the vertical system presented an almost constant
416 melting rate. Moreover, the comparative analysis showed that horizontal system provided better thermal
417 performance in melting process than vertical system. During solidification process, the natural convection
418 dominated the heat transfer at first, which rapidly reduced the temperature of PCM to its freezing point. The

heat transfer was dominated by conduction as the PCM started to solidify around the HTF tube. Due to low thermal conductivity of PCM, the solidified PCM started behaving like insulating medium and thus it reduced the phase transition rate. Due to buoyancy, the liquid PCM was moving to the upper portion of container, whereas the solidification rate was faster in lower portion. Furthermore, the comparative analysis showed that the horizontal and vertical orientations had insignificant influence on solidification rate as the average temperature and solidification rate were almost same for both cases, as shown in Fig. 11. Similarly, Allen et al.[63] experimentally analysed the influence of cylindrical container inclination on solidification rate of n-Octadecane. It was observed that due to conduction dominated heat transfer, the orientation of cylindrical container had a minimal impact on the solidification rate of PCM.

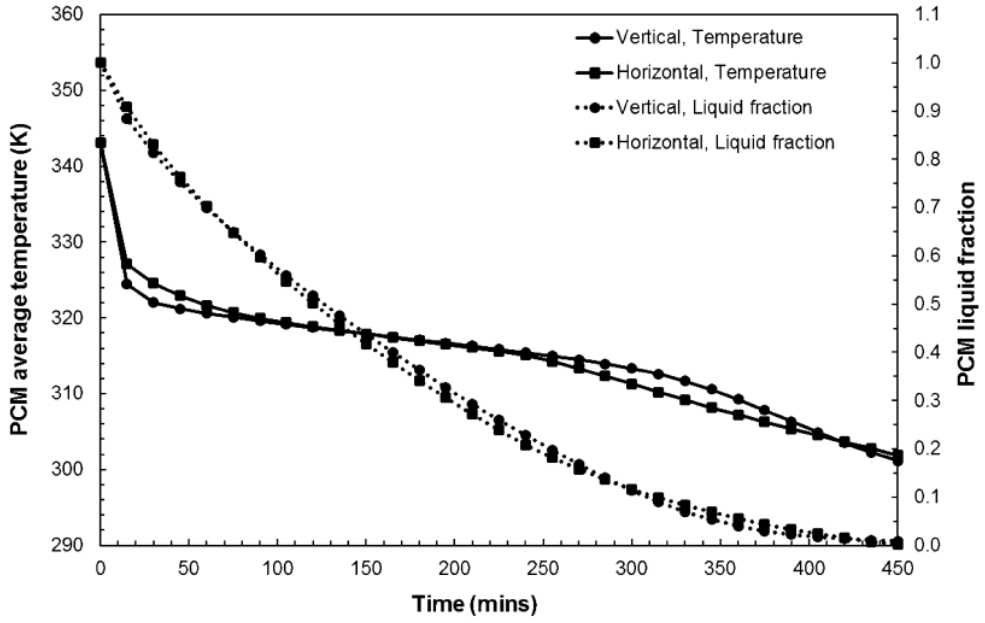

Fig.11. Comparison of PCM average temperature and liquid fraction in horizontal and vertical orientations of shell and tube container during solidification process [62]

In this section, the phase transitions of PCMs in various containers have been reviewed. It is noticed from review that conduction heat transfer and natural convection are responsible for melting behaviour of PCMs in containers with different shapes. In early stages of phase transition from solid to liquid, conduction plays a vital role in transferring excess amount of heat and is responsible for higher melting rate. Later, buoyant forces overcome viscous forces and buoyant forces driven flow depends on heat supply, operating conditions, thermo-physical properties of PCMs and container geometry. Container orientation and geometric parameters have great impact on the melting behaviour of PCMs, such as aspect ratio of rectangular and cylindrical containers,

spherical capsules radius and annular cavity eccentricity. Therefore, the selection of PCM container shall be carried with great attention, knowing the effect of geometry configuration on phase transition behaviour of PCM.

4.2 Heat exchanger surface area enhancement

Extended surfaces and fins are employed in the heat exchanger to increase the heat transfer surface area. Fins configuration and orientation play an important role in improving the performance of LHS system. Fins are normally installed in lower heat transfer coefficient side because the fins efficiency rises with declination in heat transfer coefficient. Therefore, fins are mostly on the PCM side.

Akhilesh et al. [64] numerically investigated the effect of adding more fins in rectangular container, heated from top wall. It was observed that heat transfer area and thermal energy storage were increased by increasing number of fins per unit length. However, thermal storage performance could not be enhanced any further upon increasing the number of fins beyond a critical value. Gharebaghi and Sezai [65] studied the effect of fins in rectangular container of PCM. It was noticed that inclusion of fins increased the heat transfer rate. They also reported that horizontal fins with vertical heated walls provided double heat transfer rate to that of vertical fins with horizontal heated walls. Thermal storage performance was enhanced by increasing the number of fins and reducing the gap in-between fins. However, increase in number of fin beyond the critical value could not provide considerable enhancement.

Lacroix and Benmadda [66] simulated the melting rate of PCM in rectangular container with horizontal fins and vertical heated walls. The simulation was focused on investigating the effect of number of fins and their length. It was concluded that large number of shorter fins (19 fins, each of 0.01m length) are less efficient in improving the melting rate than few number of longer fins (4 fins, each of 0.03 m length). Even with small temperature gradient, longer fins could improve the performance and it was found more efficient than increasing the heated wall temperature.

Shatikian et al. [67] numerically studied the effect of fin thickness on melting rate. It was reported that thicker fins experienced uniform temperature along the length of the fin, whereas thinner fins showed temperature gradient. Temperature uniformity was desirable for better heat transfer but too thick fins would reduce the storage capacity of container. Therefore, the thickness and number of fins should be optimized for better performance of LHS system.

Stritih [68] experimentally investigated the fin effectiveness of rectangular container. Fin effectiveness is defined as the ratio between heat flux with fins and heat flux without fins. It was noticed that heat flux with fins was high and because of that fin effectiveness was high and resulted in 40% reduction in phase transition time.

Tao and He [69] numerically examined the effect of number of fins, fin thickness and fin height on melting rate of PCM in horizontal concentric tube. It was noticed that an increase in fins number, thickness and height amplified the thermal conductivity in lower portion of PCM causing enhanced heat transfer rate and melting rate. However, excessively large number of fin, thickness and height would decrease the storage capacity of PCM. Therefore, the recommended values for number of fins, dimensionless thickness and dimensionless height were 7, 0.1 and 0.8, respectively.

Vertical fins effect with constant temperature horizontal wall on solidification time of high temperature PCM was simulated by Guo and Zhang [70]. It was observed that without fins the solidified front only moved in vertical direction, whereas with fins, simultaneous vertical and horizontal movement of solidified front was noticed. Solidification time observed linear declination with number of fins. Thermal energy discharge time was $1/30^{th}$ with fins to that without fins. Prior to critical value for fin thickness, it was observed that increasing fin thickness could decrease solidification time.

Lacroix [71] numerically studied the behaviour of LHS unit with shell and annular finned tube configuration, with PCM stored in shell side and HTF flowing in tube. Natural convection was considered by including effective thermal conductivity of PCM in conduction equation, as a function of Rayleigh number. It was concluded that annular fins enhanced the heat conduction for all values of mass flow rates and inlet temperatures. Maximum improvement in heat conduction was observed with moderate flow rate and small inlet temperature; whereas even with more number of fins, the increase in heat conduction was less significant with larger flow rate and inlet temperature. Similarly, Zhang and Faghri [72] studied the same shell and annular finned tube system and reported that fins proved to be very effective in tackling the depletion in performance caused by subcooling of PCM.

Rahimi et al. [73] experimentally examined the effect of flow rate, inlet HTF temperature and fin pitch on melting and solidification rate of R35 paraffin in fin and tube heat exchanger. An increase in flow rate from 0.2 L/min to 1.6 L/min enhanced turbulent nature of HTF and it resulted in improved melting rate, whereas the solidification rate was not affected significantly. Similarly, an increase in inlet temperature of HTF from 50 ^{o}C to 60 ^{o}C enhanced melting time, whereas, the enhancement was not impressive when inlet temperature was

increased from 60 °C to 70 °C. It was noticed that solidification rate was more enhanced as compared to melting rate with employing fins. For 5mm fin pitch, the melting and solidification time decreased from 290 to 190 minutes and from 445 to 245 minutes, respectively. Increasing the fin pitch from 5mm to 15mm could not produce a significant difference in transition rates.

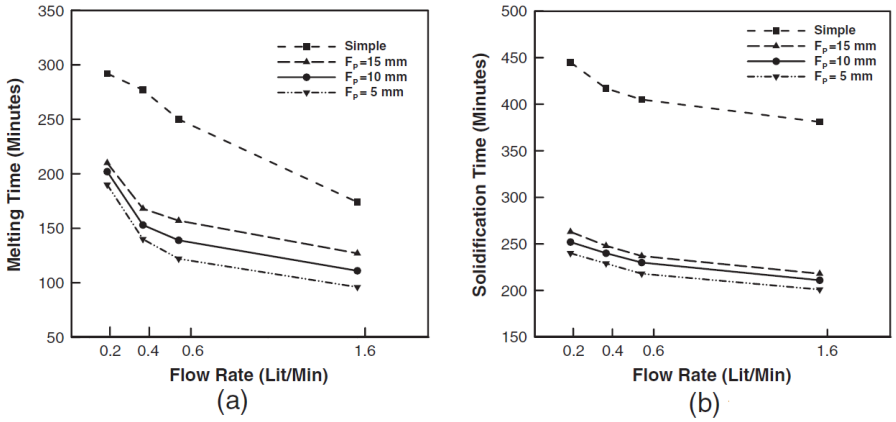

Fig.12. Effect of mass flow rate on phase transition rates for various fin pitch values: (a) melting rate and (b) solidification rate [73].

Choi and Kim [74] experimentally investigated the radial fins effect on solidification time of PCM in cylindrical container. Due to radial fins, enhancement in both radial and axial heat conduction were observed, which result in better heat recovery. It was also reported that at lower mass flow rate of HTF, solidification front was only found on fins portion nearby tube wall. Whereas for higher flow rate of HTF, solidified front was found on large fin portion and better utilization of fins could be made.

Velraj et al. [75] experimentally verified the increase in solidification rate of PCM in vertical concentric double tube, with PCM stored in inner tube with longitudinal fins. It was reported that the portion of liquid PCM which was at furthest from heat transfer surface could be covered by using longitudinal fins, which results in minimal resistance and higher thermal contact. It was noticed that increasing the number of fins in large tube was more effective and solidification time was $1/n^{th}$ times with fins to that without fins.

Rathod et al. [76] analysed the performance enhancement of LHS system by installing three longitudinal fins in shell and tube arrangement. It was noticed that an increase in inlet temperature of HTF is more effective than mass flow rate of HTF. Due to installation of fins, the melting time percentage decrease was 12.5% and 24.52% for the inlet temperature 80 °C and 85 °C, respectively. Similarly, the percentage decrease in solidification time was reported to be 43.6%.

517 An experimental study was carried by F. Agyenim et al. [77], to compare the thermal performance of
518 erythritol in various geometric configurations of horizontal concentric tube, such as concentric tube without fins,
519 with radial fins and with longitudinal fins. PCM charging cycle was carried out for 8 hours. It was reported that
520 only longitudinal fin configuration has completely melted the PCM. During the discharging cycle, longitudinal
521 fin configuration showed insignificant subcooling. Therefore, the longitudinal fin configuration was
522 recommended for enhanced performance in concentric tube LHS system.

523 Medrano et al. [78] experimentally investigated the melting and solidification rate of organic PCM RT 35
524 in five commercially available heat exchangers. It was noticed that double pipe heat exchanger and plate type
525 heat exchanger are not appropriate to be used as PCM containers. However, the double pipe with graphite
526 matrix, double pipe with fins and compact heat exchanger can be utilized as heat storage containers. It was
527 reported that compact heat exchanger produced highest average thermal power i.e. 1kW for both melting and
528 solidification case. The normalized thermal power was found maximum in double pipe with graphite matrix, in
529 range of 700–800 W/m^2–K.

530 As discussed, the inclusion of fins in LHS system enhances the storage performance and reduces the
531 phase transition time. The number and size of fins play an important role in LHS system performance and
532 promotion of natural convection. External fins have more impact on LHS system performance during
533 solidification process than melting process. It is because melting process is dominant by convection, whereas
534 solidification is governed by conduction. In addition, the number of fins in a LHS system can affect the thermal
535 storage capacity of container due to small volume for PCM. Therefore, the fins number and size should be
536 optimized for the system thermal performance enhancement and thermal energy storage capacity.

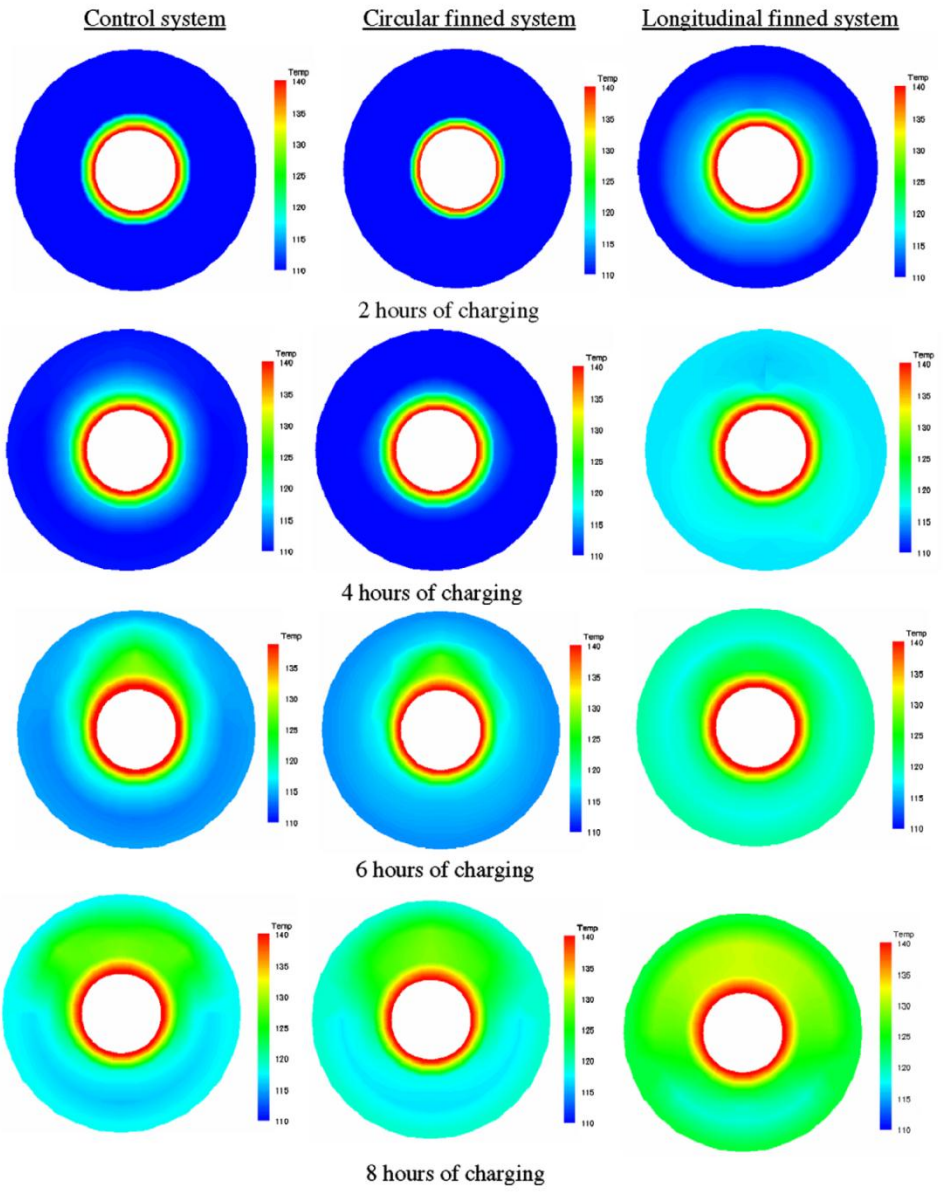

Fig.13. Comparison of thermal performance of erythritol in various geometric configurations: (i) Control system (no fins), (ii) Circular finned system and (iii) Longitudinal finned system [77].

4.3 PCM additives to increase the thermal conductivity

Despite the fact that PCMs possess higher thermal storage density, the slower rate of melting and solidification limits the potential practical applications of LHS system. This is due to lower thermal conductivity of both organic and inorganic PCMs which ranges from 0.1 to 0.7 W/mK, as shown in Table 3 and Table 4. In recent years, a subchapter of a book by Mehling and Cabeza [20], and portions of few review papers [52, 53, 79, 80] are published on this topic. However, this section thoroughly reviews the latest research developments in thermal conductivity enhancement of both paraffins and salt hydrates by using metal matrices and structures,

expanded graphite, metal nanoparticles and carbon fibers. This section is focused on effect of addition of additives on thermal conductivity, latent heat storage capacity and transition rate of PCMs.

Melting and solidification rate can be enhanced by adding naturally available materials such as graphite, carbon fibers, copper, aluminium, metal matrices etc. Copper matrices enhanced the thermal conductivity of paraffin by approximately 80% as compared to aluminium matrices. Moreover, diamond coated copper matrices can further increase the thermal conductivity [81].

Mesalhy et al. [82] performed a numerical parametric study to identify the effects of employing solid matrices with different porosities of 0.85, 0.90 and 0.95; and thermal conductivity ratios on thermal performance of paraffin based LHS system. Thermal conductivity ratio, ks/kf ranged from 50-200. The term ks and kf represented the thermal conductivity of solid porous matrix and PCM, respectively. It was reported that thermal performance of LHS system was dependent on both porosity and thermal conductivity of employed matrix. Compared to pure paraffin, the addition of porous matrix increased the rate of melting and heat transfer rate. A decrease in matrix porosity resulted in increased thermal conductivity and melting rate of paraffin but it also dampened the convection motion. It was suggested that a matrix with high thermal conductivity and high porosity can enhance the storage performance in best way.

Due to high thermal conductivity and absorbability of graphite, it is used by many researchers as an additive in LHS system to improve thermal performance. Thermal conductivity of graphite ranges from 24 to 270 W/mK. Haillot et al. [83] characterized and elaborated composites of expanded graphite and several PCMs and reported an increase of thermal conductivity from 0.2 – 1 W/mK for pure PCM to 5 – 50 W/mK for composite. However, the inclusion of expanded graphite to RT-65 paraffin decreased the latent heat capacity from 170 – 140 kJ/kg. It showed that thermal capacity and thermal conductivity of LHS system depended on the amount of expanded graphite in composite.

Similarly, the effect on melting time, thermal conductivity and thermal capacity on composite of n-docosane (paraffin) and different mass fractions of expanded graphite is investigated by Sari and Karaipekli [84]. Liquid paraffin absorbed in pores of expanded graphite of 2%, 4%, 7% and 10% mass fraction, making a form-stable composite with no leakage due to capillary force and surface tension of expanded graphite. The density of 10% expanded graphite composite was less than pure paraffin. The increase in mass fraction of expanded graphite showed an increase in thermal conductivity but a decrease in thermal capacity. An optimum

mass fraction of 10% expanded graphite resulted in four time increased thermal conductivity, causing about 32% reduction in melting time, and a small drop in thermal capacity from 194.6 - 178.3 kJ/kg.

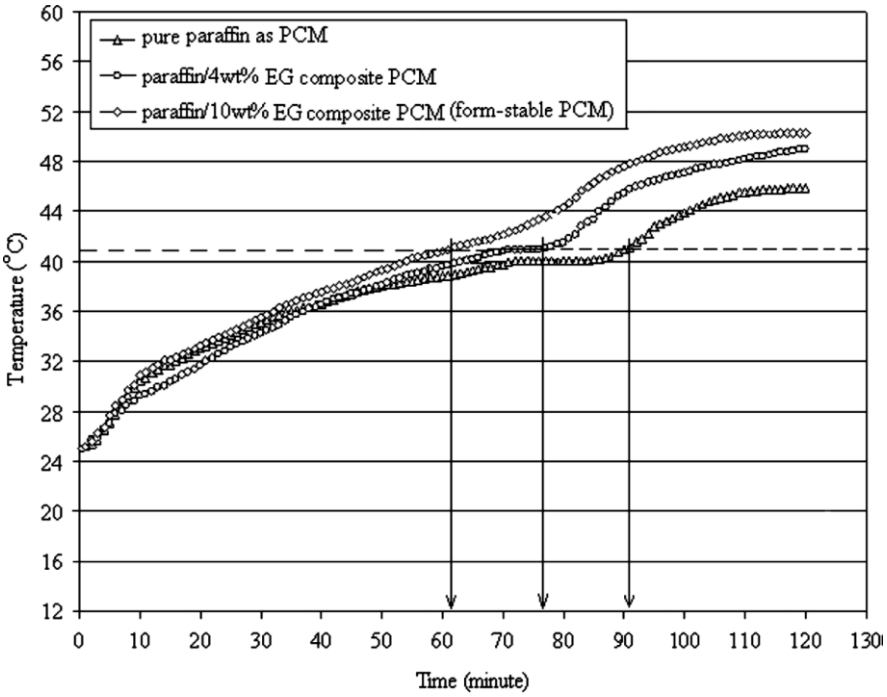

Fig.14. Melting time of pure paraffin and composite paraffin/EG [84].

An experimental investigation on thermal conductivity enhancement of $CaCl_2.6H_2O$ and expanded graphite composite was conducted by Z. Duan et al.[85] . OP-10 was added as a surfactant to improve the bonding energy and sealing performance of the composite. Various samples were prepared with expanded graphite mass fraction of 50%, 40%, 30%, 20% and 10%. DSC results showed that composite sample with 40% mass fraction of expanded graphite produced comparatively higher latent heat of fusion (145 kJ/kg), whereas sample of 50% mass fraction of expanded graphite provided lower latent heat of fusion (49.10 kJ/kg). TG analysis of composite samples evidently showed that the inclusion of OP-10 surfactant enhanced the thermal stability. Moreover, thermal constant analyser tests presented that that 50% mass fraction of expanded graphite improved the thermal conductivity of $CaCl_2.6H_2O$ (8.796 W/mK) by 14 times to that of pure $CaCl_2.6H_2O$ (0.596 W/mK).

Thermal performance enhancement of $Na_2SO_4.10H_2O$ and $Na_2HPO_4.12H_2O$ with expanded graphite was examined by Y. Wu and T. Wang [86]. Impregnation and physical blending techniques were used to prepare the composite sample of 3.5g of each salt hydrates with 1g of expanded graphite. The composite sample was coated with 0.2g of paraffin wax to restrain salt hydrates from phase segregation. It was reported that the composite

sample demonstrated good thermal stability after 100 thermal cycles and presented good latent heat of fusion (172.3 kJ/kg). Moreover, the inclusion of expanded graphite increased the thermal conductivity of hydrated salts to 3.643 W/mK.

H.K. Shin et al.[87] investigated the thermal performance enhancement of sodium acetate trihydrate by inserting various weight percentages of expanded graphite. Carboxymethyl cellulose (CMC) was added as a thickening agent. It was reported that the PCM composite containing 2.5 wt% of expanded graphite and 5 wt% of thickening agent exhibited a high thermal conductivity of 1.85 W/mK and excellent thermal stability. On the contrary, the same PCM composite sample with 5 wt% of graphite powder (particle size $\leq$ 50 μm) and 5 wt% of CMC was prepared and investigated by M. Dannemand et al.[88]. The maximum thermal conductivity of composite was reported to be 1.1 W/mK.

The results from various research shows that graphite is an excellent additive to enhance thermal performance of LHS system. However, its porosity plays a vital role in effectiveness of improved thermal performance. If the composite of small mean pore size graphite is selected then it may cause difficulty in impregnation of PCM in porous media of graphite and hinders the molecular moment, which can decrease the latent heat capacity. On the contrary, if the mean pore size is increased then it can cause leakage problem as reduction in capillary forces. Moreover, the composite of graphite and PCM can be prepared by using chemical or mechanical processes, which are time and energy consuming. Therefore, to avoid these shortcomings, another simple technique to enhance thermal conductivity is dispersion of high thermal conductivity particles.

An experimental study was conducted on thermal conductivity enhancement of paraffin wax by incorporating aluminium particles of 80 μm, with a mass fraction of 0.1, 0.3, 0.4 and 0.5, by Mettawee and Assassa [89]. Mass fraction was the ratio of mass of aluminium powder to mass of compound of paraffin wax and aluminium powder. During charging time, the heat transfer from solar collector to paraffin wax/aluminium composite was increased as the mass fraction increase from 0.1 to 0.5. However, the increase in mass fraction beyond 0.5 resulted in insignificant increase in heat transfer rate. For aluminium mass fraction of 0.5, the thermal conductivity of composite increased and produced 60% reduction in charging time as compared to pure paraffin wax. Similarly for discharging process, the composite of 0.5 mass fractions showed more homogenous solidification. The highest mean daily efficiency of the LHS system increased from 54.8% for pure paraffin wax to 94% for composite.

Performance enhancement of 1-tetradecanol (TD) and silver nanoparticle composite was investigated by Zeng at al. [90], using TG-DSC, IR, TEM, XRD and thermal conductivity evaluation method. The investigated composite samples were based on various mass fractions of 0.98, 0.94, 0.80, 0.50, 0.20 and 0.06. Mass fraction was the ratio of mass of pure TD to the combined mass of TD and silver nanoparticles. It was reported that thermal conductivity of composite increased with increase in the amount of silver nanoparticle. Thermal conductivity enhancement was examined by the increase in temperature at particular time. It was noticed that after 150 seconds of melting process, the pure TD was at 26 ^{o}C, whereas the composite of mass fraction of 0.06 was at 30 ^{o}C. Also, no interaction between TD and silver nanoparticle was noticed and the stability of composite was found to be almost the same as to that of pure TD. However, thermal storage capacity of composite decreased with increase in silver nanoparticle (234.2 kJ/kg for pure TD, 216.5 kJ/kg for composite of mass fraction of 0.98 and 119.4 kJ/kg for composite of mass fraction of 0.50, respectively) and the phase transition temperature was also reduced as compared to pure TD.

To improve the thermal conductivity of paraffin, various techniques such as vertical cylinder with internal longitudinal fins, lessing rings and bubble agitation are studied by Velraj et al. [91]. In case of lessing rings, hollow steel rings of 1 cm diameter were added in cylindrical paraffin container. Reduction in solidification time was reported for both fins and lesser rings based LHS system. It was found that solidification time for fins and lesser rings were $1/4^{th}$ and $1/9^{th}$ that of plain tube LHS system, respectively. However, the inclusion of fins and lesser rings occupied 7% and 20% of total storage volume of container respectively and thus reducing the storage capacity of LHS system, as shown in Fig. 15. Therefore for large container size of LHS system, lesser rings will perform better than fins.

Due to higher density of metal particles and metal structures, there is a possibility that the additives can settle at the bottom of container and increasing the weight of container. As discussed in section 3.2, there are compatibility concerns between metals and PCMs. Therefore, researchers have been searching for low density but high thermal conductivity additives, which are compatible with all PCMs. Carbon fibers is much lighter as compared to metal particles and its thermal conductivity is almost equal to copper and aluminium. Also, it has a good corrosive resistant nature and possesses good compatibility with almost all PCMs, thus it can qualify for better alternative to improve thermal performance of LHS system. Elgafy and Lafdi [92] analytically and experimentally investigated the performance enhancement of Paraffin wax based LHS system by adding carbon nanofibers of 100nm outer diameter and 20µm average length. Samples of different mass ratio (1%, 2%, 3% and

4%) of carbon nanofibers were made using shear mixing and melting process. The composite showed an almost linear increase in thermal conductivity and output power with increase in mass ratio of carbon nanofibers, which resulted in increased solidification rate and insignificant reduction in storage capacity. The solidification time was reduced by 23% by using 1% mass ratio of carbon nanofibers. It was reported that further improvement in thermal performance can be achieved by uniform distribution of fibers.

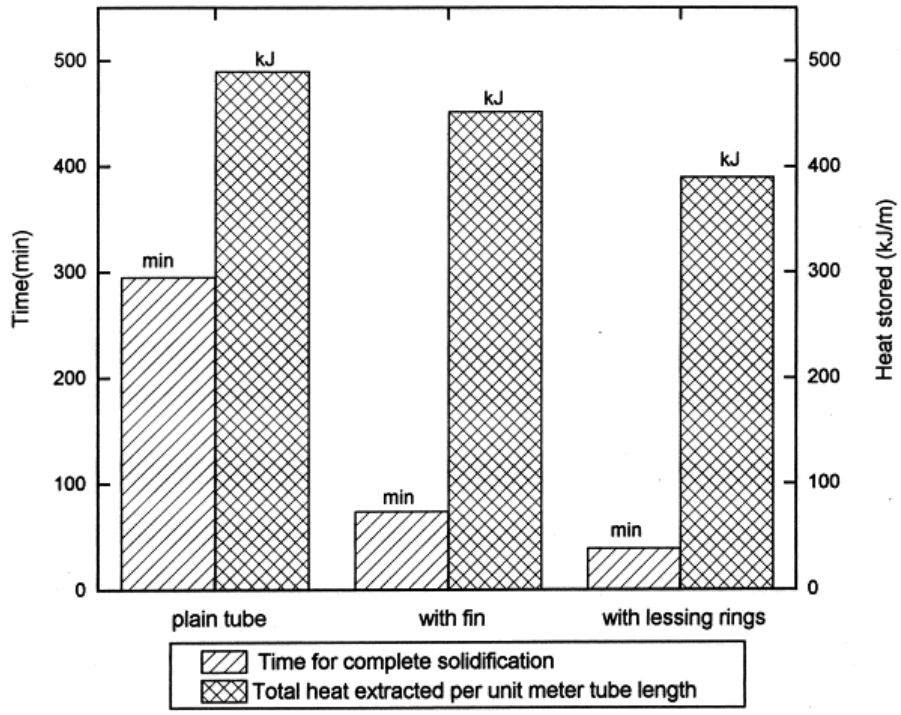

Fig.15. Solidification time and total heat storage capacity for various configurations [91].

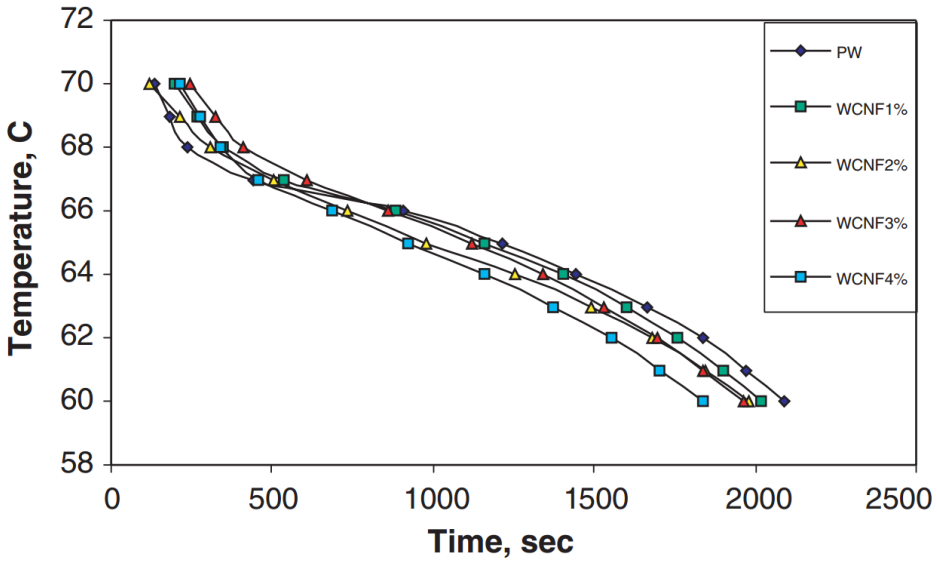

Fig.16. Solidification temperature with respect to time for various mass ratios of Carbon nanofibers [92].

Fukai et al. [93] inspected the effect of randomly and uniformly oriented carbon fibers on the thermal performance enhancement of paraffin wax based LHS system. Carbon fibers of 10μm diameter, 220 W/mK thermal conductivity and 2170 kg/m^3 density were packed with paraffin wax in a steel cylindrical capsule. It was found that effective thermal conductivity of uniformly oriented brush type was three times to that of randomly oriented type. Moreover, in case of small mass fraction of carbon fibers, the randomly oriented carbon fibers dampened the natural convection and thus resulted in lower melting rate than pure paraffin. Whereas, the higher melting rate in brush type orientation was not affected by loss in convection. Similarly, Fukai et al. [94] experimentally and numerically investigated the effect of inclusion of carbon fiber brushes in paraffin wax based LHS system. It was reported that an enhancement of 20% and 30% in charging and discharging respectively was achieved as compared to normal paraffin wax.

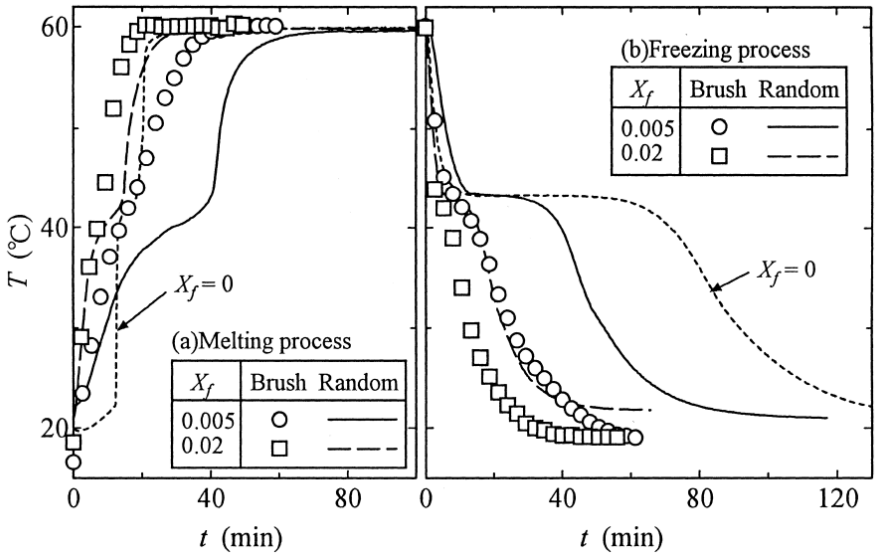

Fig.17. Transient temperature response to random type and brush type orientation of carbon fibers [93].

As reviewed in this section, the thermal conductivity of LHS system can be increased significantly by incorporating high conductivity additives and it can enhance the melting and solidification rate. However, the addition of additives can reduce the storage volume of PCM and it can lead to loss in storage capacity. Thus, an optimum mass of additives should be selected for enhancing thermal performance.

4.4 Multiple PCMs method

Instead of single PCM, using multiple PCMs technique has reported an increase in LHS system performance and storage capacity. During the charging and discharging process of the LHS system, the rate of heat transfer depends largely on the temperature difference between PCM melting temperature and HTF

temperature. In single PCM case, the temperature of HTF decreases along the length of flow which results in temperature difference reduction. As a consequence, the rate of heat transfer decreases and therefore the LHS capacity reduces and most part of stored thermal energy is sensible energy. Whereas in multiple PCMs case, the storage medium consist of different PCMs in descending order of their melting temperatures, even if the temperature of HTF decreases the unit maintain almost a constant temperature difference. Multiple PCMs method yields constant heat flux to the PCM in melting process and to the HTF in solidification process.

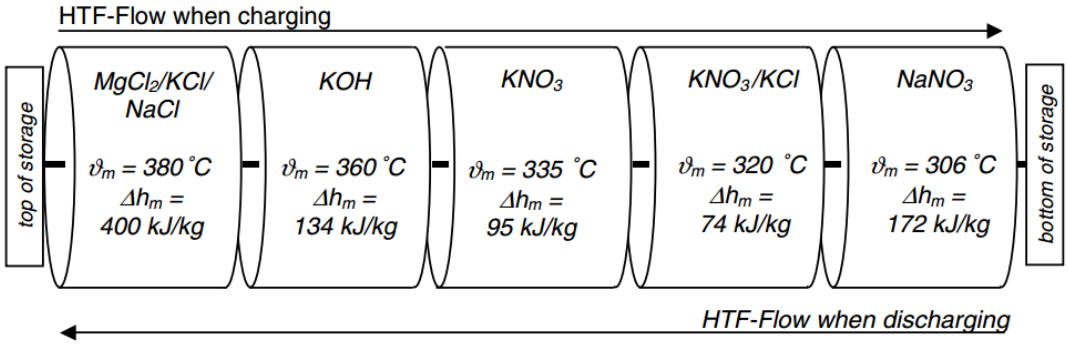

Fig.18. A schematic of multiple PCMs based LHS unit [95].

Wang et al [96] numerically investigated the performance enhancement of LHS system by employing multiple PCMs (PE, PG and NPG). It was suggested that an increase in number of PCMs would reduce the phase transition time. Numerical results indicated that phase transition for all PCMs were almost homogenous and with constant rate.

Mosaffa et al [97] numerically investigated the improved performance of free cooling system using multiple PCM based LHS system. The PCMs selected for investigation were $CaCl_2.6H_2O$, Paraffin C18 and RT25. Energy based optimization were used to find out the effect of length and thickness of PCM slab, and fluid passage gap on storage performance. It was reported that $CaCl_2.6H_2O$ and RT25 composite was very effective in maintaining the outlet air temperature below 27 ^oC for 8 hours and providing maximum heat absorbing capacity.

Gong and Mujumda [98] developed a one dimensional finite element heat conduction phase change model for melting and freezing processes of composite PCMs slabs. The model was used to investigate the performance of various arrangements of PCMs with descending order of their melting temperatures, thermo-physical properties and various boundary conditions for both melting and heating processes as shown in Table 6. E_T and E_M represent the actual energy stored or retrieved in a cycle and maximum energy stored or retrieved, respectively. The ratio between E_T and E_M represents the LHS system performance. Upon reaching to steady

reproducible state, the multiple PCM slab resulted in enhanced melting and solidification rate as compared to single PCM slab. The charge and discharge rate was enhanced from 21.9% to 31.7% by decreasing the thermal conductivity ratio from 1.0 to 0.1, and the percentage enhancement was decreased by periodic reduction in thermal diffusivity ratio. Increase in latent heat of multiple PCMs resulted in improved charge and discharge rate. It can also be observed from the table 6 that the melting and solidification rate can be enhanced by minimizing the temperature differences between boundary temperatures using multiple PCMs.

Table 6

Performance enhancement using multiple PCM [98]

	Property	**$t_m=t_s$ (s)**	**Slab type**	**E_T (J/m^2)**	**E_T/E_M**	**Enhancement (%)**
Case	Thermal conductivity kl/ks					
1	1	650	Single	404,508	0.632	
			3-PCM	493,178	0.771	21.9
2	0.4	1150	Single	439265	0.774	
			3-PCM	534425	0.941	21.7
3	0.2	1950	Single	415613	0.764	
			3-PCM	517257	0.969	26.9
4	0.1	3375	Single	393120	0.723	
			3-PCM	517790	0.955	31.7
Case	Thermal diffusivity al/as					
1	1	650	Single	404508	0.632	
			3-PCM	493178	0.771	21.9
2	0.4	800	Single	552627	0.674	
			3-PCM	627102	0.765	13.5
3	0.2	1000	Single	704900	0.629	
			3-PCM	758942	0.678	7.67
Case	Latent heat (J/kg)					
1	2000	375	Single	263161	0.598	
			3-PCM	304540	0.692	15.7

2	4000	650	Single	404508	0.632	
			3-PCM	493178	0.771	21.9
3	8000	1200	Single	754818	0.726	
			3-PCM	945164	0.909	25.2
4	16000	2150	Single	1329710	0.723	
			3-PCM	1756840	0.955	32.1
Case	Temperature swing (^{o}C)					
1	T_{wm}= 80, T_{m}= 70, T_{wf}= 60	1750	Single	363228	0.757	-
2	T_{wm}= 80, T_{m1}= 75, T_{m2}= 70, T_{m3}= 65, T_{wf}= 60	1750	3-PCM	457240	0.953	25.9
3	T_{wm}= 120, T_{m}=90, T_{mf}= 60	650	Single	404508	0.632	-
4	T_{wm}= 120, T_{m1}= 105, T_{m2}= 90, T_{m3}= 75, T_{wf}= 60	650	3-PCM	493178	0.771	21.9
5	T_{wm}= 160, T_{m}= 110, T_{wf}= 60	400	Single	465331	0.582	-
6	T_{wm}= 160, T_{m1}= 135, T_{m2}= 110, T_{m3}= 85, T_{wf}= 60	400	3-PCM	545623	0.682	17.3
7	T_{wm}=200, T_{m}= 130, T_{wf}= 60	350	Single	579027	0.603	-
8	T_{wm}= 200, T_{m1}= 165, T_{m2}= 130, T_{m3}= 95, T_{wf}=60	350	3-PCM	670265	0.698	15.8

708

709 Farid and Kansawa [99, 100] numerically and experimentally studied the performance enhancement of
710 LHS system by employing three commercial waxes of different temperatures (44 ^{o}C, 53 ^{o}C and 64 ^{o}C) and
711 reported an increase of 10-15% in heat transfer rate to that of single PCM unit. It was also reported that the
712 phase transition of all PCMs started simultaneously.

713 Aldoss and Rahman [101] investigated the improvement in performance of multiple paraffins based LHS
714 system by increasing the number of stages. Spherical capsule containing paraffin 40, paraffin 50 and paraffin 60
715 were used in various stages along the length of bed. It was observed that an increase in number of stages of

multiple paraffins based LHS system resulted in enhanced rate of charge and discharge, increased heat transfer rate and improved storage capacity. However, increasing the number of stages more than three could not enhance the system significantly.

Wang et al [102] experimentally investigated the decrease in melting time of LHS unit consisting of three coaxial cylindrical containing stearic acid, sliced paraffin and lauric acid, respectively. LHS unit was dipped in water and experiments were conducted for different temperatures, for both multiple PCMs unit and single PCM (sliced paraffin) unit. The experimental results demonstrated that charging rate of multiple PCMs unit was enhanced and resulted in 37-42% reduction in melting time compared to single PCM.

4.5 PCM encapsulation

PCM encapsulation is a process of shelling the PCM with suitable coating material to keep it isolated from surrounding. The encapsulation process was invented by Barrett K Green in 1940s. Encapsulation ensures the sustainability of true composition of PCM that can be altered by connection with surrounding, reduces the possibility of surrounding reaction with PCM, improves thermal and mechanical stability, improves heat transfer rate and compatibility with hazardous PCMs that cannot be exposed to surrounding such as building temperature control, food storage and blood transport applications. Encapsulation of organic PCMs is given preference over salt hydrates for its non-corrosive nature and insignificant solubility in water. However, the inflammable nature of organic materials can be controlled by using inorganic coating materials. As shown in Fig. 19, chemical and physical are two broad manufacturing methods of PCM encapsulation. Physical encapsulation methods deal with large amount and rough surface encapsulation as compared to chemical techniques. Chemical encapsulation techniques result in better heat storage capacity than that of physical methods. In-situ polymerization manufacturing technique with its smaller capsule size and excellent shell structure is preferred over others techniques. PCM encapsulation can be also be classified by different sizes such as macro, micro and nano encapsulation and various container shapes as spherical, cylindrical, tubular or rectangular. In last decade, several review articles and subchapters of books are published on this topic. Review articles on nanoencapsulation [103, 104] and microencapsulation [3, 105-107] are focused on various encapsulation types, techniques and applications. Similarly, the subchapters of books by Cabeza [20, 108] are focused on macro and micro encapsulation. This section reviews the updated research on thermal performance enhancement and thermo-physical stability of micro and macro encapsulated PCMs. This section is focused on effects of

encapsulation on thermo-physical stability, latent heat storage capacity, thermal conductivity and phase transition rate.

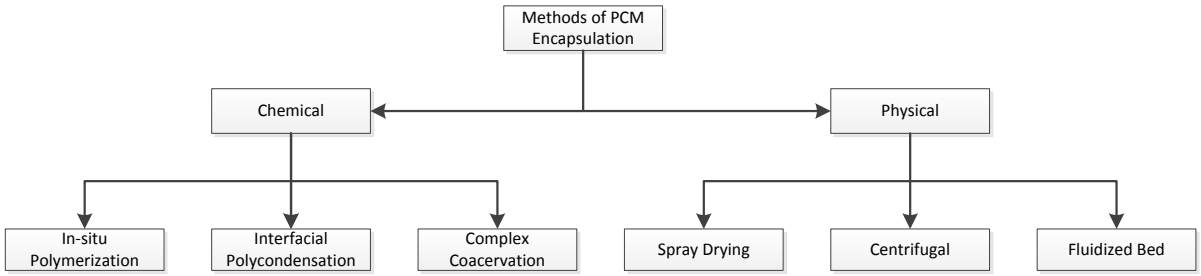

Fig.19. Various methods of PCM encapsulation.

4.5.1 Microencapsulation

Mechanical strength of encapsulated PCM can be identified by the core to coating ratio. An increase in core to coating ratio proceeds in deteriorating coating strength and increases possibility of PCM leakage from encapsulation, while a decrease in core to coating ratio can reduce the amount of PCM in encapsulation. Ohtsubo et al. [109] examined the mechanical stability of microcapsules by using mass median diameter factor (D) and wall thickness factor (T). It was noticed that for larger ratio of D and T, a smaller pressure is enough to break 50% of coating material of encapsulation. Zhang and Wang [110] synthesized microencapsulated PCM with n-octadecane as core material and polyurea as coating material. Core to coating ratio of 70/30 and 75/25 were examined, with mean particle size of 6.9 µm and 7.1µm, respectively. Lower core to coating ratio (70/30) produced better thermal stability, while the higher core to coating ratio (75/25) caused slippage of PCM at 200 ^{o}C.

Namwong et al. [111] investigated the latent heat capacity of microencapsulated PCM with octadecane as core material and divinylbenzene and methyl methacrylate (DVB-MMA) polymer as coating material. The average diameter of microcapsule was 3.2 µm. Three polymer samples were tested. The samples contained different percent weights of DVB and MMA such as 100:0, 50:50 and 30:70 wt%, respectively. The latent heat of all samples of microencapsulated PCM was reported to be 189 kJ/kg, 218 kJ/kg and 223 kJ/kg, respectively. It was observed that the latent heat of microencapsulated PCM increased as the percent weight of hydrophilic MMA increased to 70 wt%. Yu et al. [112] examined the thermal conductivity enhancement of microencapsulated n-octadecane. $CaCO_3$ was used as shell material. The spherical microencapsulated PCM was having a diameter of 5 µm. Three samples of various percent weights of core and shell material were tested such as 30:70, 40:60 and 50:50 wt%, respectively. Thermal conductivity of pure n- octadecane was 0.153 W/mK. It

was reported that thermal conductivity of all samples of microencapsulated PCM improved to 1.674 W/mK, 1.325 W/mK and 1.264 W/mK, respectively. Also, the microencapsulated PCM samples were subjected to 200 thermal cycles and it showed a good thermal stability and structural reliability. Yang et al. [113] examined the performance enhancement of thermo-physical properties of microencapsulated n-octadecane. Silicon nitride and polymethyl methacrylate polymer was used as shell material. Four samples of microencapsulated PCM were tested. The percent weight of core materials ranged from 82.3 - 66.4 wt%. It was noticed that latent heat of fusion reduced from 151.30 - 122.07 kJ/kg as the percent weight of core material decreased from 82.3 - 66.4 wt%. However, the mechanical strength of sample with 66.4 wt% of core material appeared to be four time higher (16.24 mN) than ordinary PCM.

Sarier et al.[114] evaluated the thermal performance enhancement of two microencapsulated PCMs with n-hexadecane and n-octadecane as core materials. Urea-formaldehyde was used as coating material. Silver nanoparticles were added to core materials to improve the thermal performance of microencapsulated PCMs. The average particle size of silver nanoparticles ranged from 163-496 nm. Six samples of microencapsulated PCMs were tested. Four samples were containing 176.6 mmol of n-hexadecane and 0, 26, 52 and 104 mmol of silver nanoparticles as core material, respectively. Likewise, two samples were containing 157.2 mmol of n-octadecane and 0 and 26 mmol of silver nanoparticles as core material, respectively. For all samples, the core to coating ratio by mass was kept constant at 1:1. It was reported that the latent heat capacity of microencapsulated n-hexadecane increased from 115-137 kJ/kg as the amount of silver nanoparticles increased from 0-52 mmol. Likewise, the thermal conductivity improved from 0.0557- 0.1231 W/mK as the amount of silver nanoparticles increased from 0-104 mmol. In case of microencapsulated n-octadecane, the latent heat capacity improved from 117-168 kJ/kg and thermal conductivity increased from 0.0695- 0.0978 W/mK with addition of 26 mmol of silver nanoparticles. The samples were also subjected to 100 thermal cycles and the results indicated a good thermal stability and durability. Jiang et al.[115] used emulsion polymerization to synthesise paraffin wax microencapsulates with methyl methacrylate-co-methyl acrylate (MMA-MA) as coating material and nano-Al_2O_3 as additives to enhance thermal performance. Six samples were evaluated with varied mass ratio of nano-Al_2O_3 (0, 5, 16, 27, 33 and 38 wt%). It was reported that thermal conductivity of microencapsulated PCM samples improved from 0.2442-0.3816 W/mK as the mass ratio of nano-Al_2O_3 increased from 0-38 wt%. However, the latent heat capacity of microencapsulated PCM decreased from 110.40-75.40 kJ/kg as the mass ratio of nano-Al_2O_3 increased from 0-38 wt%, due to drop in content of paraffin wax. It was also noticed that the microencapsulated PCM samples with nano-Al_2O_3 additives displayed better thermal stability.

Alkan et al. [116] studied the experimental preparation, characterization and calculating the thermal behaviour of microencapsulated docosan-PMMA. The microencapsulated docosane was subjected to 5000 thermal cycles and the results depicted a good thermal stability and no chemical degradation. Ma et al. [117] prepared spherical shape encapsulated paraffin-PMMA by UV irradiations to emulsion polymerization. The size of encapsulated paraffin-PMMA was 0.5 – 2 μm. Thermal stability tests were conducted for 1000 thermal cycles. The results showed a good thermal stability with melting point varied in a range of 33.40 – 35.71 ^{o}C and latent heat varied from 99.8 – 95.6 kJ/kg.

4.5.2 Macroencapsulation

Howlader et al. [118] investigated the chemical and physical stability and thermal performance of larger capsules of size (2.833 mm diameter) with paraffin as core material. It was reported that after 1000 thermal cycles, the encapsulated paraffin showed a good thermal and structural stability, and stable thermal storage capacity. Alam et al. [119] experimentally investigated the thermo-physical stability of spherical encapsulated $NaNO_3$. The diameter of hemispherical pellets of $NaNO_3$ ranged from 12.5-25.5 mm. Firstly, the PCM was encapsulated by a layer of polymer (PTFE), having a thickness of 0.5-0.7 mm. Subsequently, it was coated with a thin layer of nickel (10-80 μm). Due to polymer layer in between molten PCM and nickel, the possibility of corrosion was reduced. The capsule was subjected to 2200 thermal cycles and the results showed excellent thermo-physical stability.

Cabeza et al. [120] studied the thermal storage behaviour of solar pilot plant with several modules of encapsulated PCM-graphite. A granular compound of sodium acetate trihydrate (90 vol.%) and graphite (10 vol.%) was encapsulated in aluminium container of size 8.8 cm x 31.5 cm. As shown in the Fig. 20, the inclusion of 2, 4 and 6 PCM modules carried a weight of 2.1 kg, 4.2 kg and 6.3 kg, and it occupied 2.05 vol.%, 4.1 vol.% and 6.16 vol.% of storage tank, respectively. An increase in thermal density of 40%, 57.2% and 66.7% was noticed for 1 K temperature difference in case of 2, 4 and 6 PCM modules, respectively. Thermal density increase was 6%, 12% and 16.4% for 8 K temperature difference, respectively. The inclusion of encapsulated PCM-graphite maintained the temperature of water top layer in storage tank above 54 ^{o}C for 10-12 hours. Similarly, Mehling et al. [121] investigated the inclusion of encapsulated paraffin-graphite in brass cylinders of size 10 cm x 30 cm. Thermal storage capacity was increased by 20% to 45% and the hot water storage duration was increased by 50% to 200%.

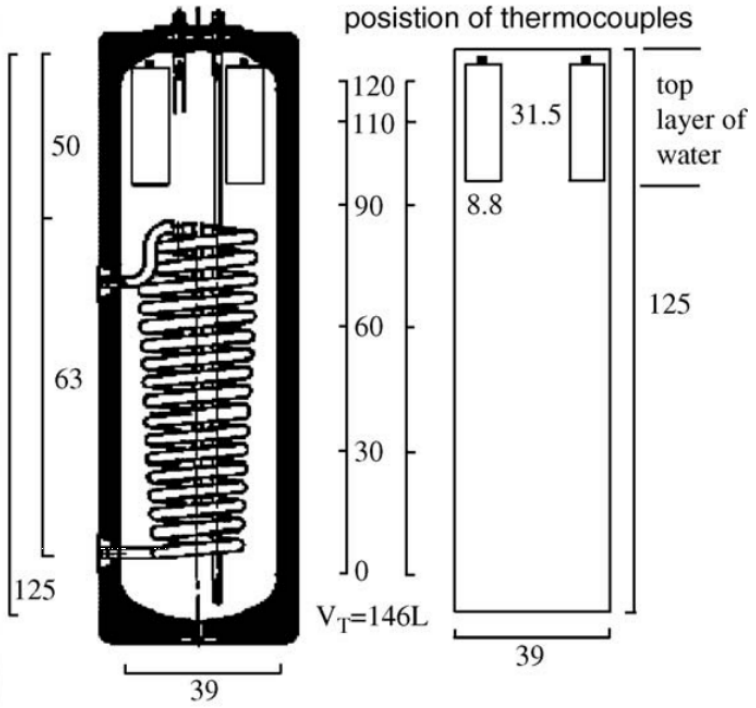

827

828 **Fig.20.** Schematic of 2 PCM modules embedded on the top portion of hot water storage tank [120].

829 Veerappan et al. [122] performed analytical study on influence of encapsulation size on melting and
830 solidification rate. It was noticed that as the diameter of capsule increased from 4 cm to 12 cm, the melt time of
831 encapsulated $CaCl_2.6H_2O$ also increased from 26 minutes to 192 minutes, respectively. Similarly, it was
832 reported that increase in capsule diameter will reduce the solidification rate and therefore the encapsulated PCM
833 will take more time to solidify as compared to small diameter. Calvet et al. [123] conducted numerical and
834 experimental examination of improvement in phase transition rate of PCM composite in a spherical
835 encapsulation. The diameter of capsule was 98mm. Graphite flakes and expanded graphite was incorporated as
836 thermal conductivity enhancement additives. It was reported that the addition of 13%wt. of graphite flakes
837 reduced both the melting and solidification time by 30% each. Whereas, the addition of 13%wt. of expanded
838 graphite reduced the melting and solidification time by 60% and 40%, respectively. Zhang et al. [124]
839 conducted numerical and experimental investigation to find the increase in solidification rate of $NaNO_3$ (60
840 wt%) and KNO_3 (40 wt%) composite in cylinder encapsulation. The capsule material was AISI 321. The outer
841 diameter and height of capsule was 75mm and 77mm, respectively. Metallic foam was inserted as thermal
842 conductivity enhancement additive. The cylindrical capsules were heated in electric furnace to melt the
843 composite PCM and then subjected to air and water to measure the solidification time. In case of air cooling, the
844 solidification time was reduced from 3600s for PCM composite with no enhancement to 2800s for PCM

composite with metallic foam. However in case of water cooling, the solidification time of PCM composite with metallic foam reduced further to 700s.

Wai et al. [125] studied the effect of capsules shape, diameter and coating thickness on thermal performance of encapsulated PCM. It was reported that spherical capsule produced an excellent heat release performance as compared to cylindrical, plate and tube type capsules. It was observed that with increase in PCM diameter from 2mm to 5mm, the heat release rate decreased. As the coating thickness increase from 0.2 mm to 0.4 mm, the mechanical stability increased but it reduced the amount of PCM in capsule and therefore it affected the thermal storage capacity. Ismail and Henriquez [126] developed a model to study the effect of spherical capsule size, coating thickness and material, initial PCM temperature on solidification rate. It was observed that coating material of high thermal conductivity and smaller capsule size with low external temperature reduced the solidification time. Increase in internal radius of spherical capsule lead to increased solidification time. As constant mass of PCM resulted in constant internal radius of 0.05m, the critical external radius for copper, PVC and glass were found to be 17.46 m, 0.003 m and 0.054 m, respectively. Increase in coating thickness could enhance solidification rate, therefore external radius of copper and glass could be increased up to their critical values, whereas, PVC critical radius was found to be lower than internal radius, thus an increase in PVC external radius would reduce the solidification rate. Ismail and Moraes [127] also observed that solidification rate could be increased by using coating material of high thermal conductivity, smaller capsule diameter and lower external temperature.

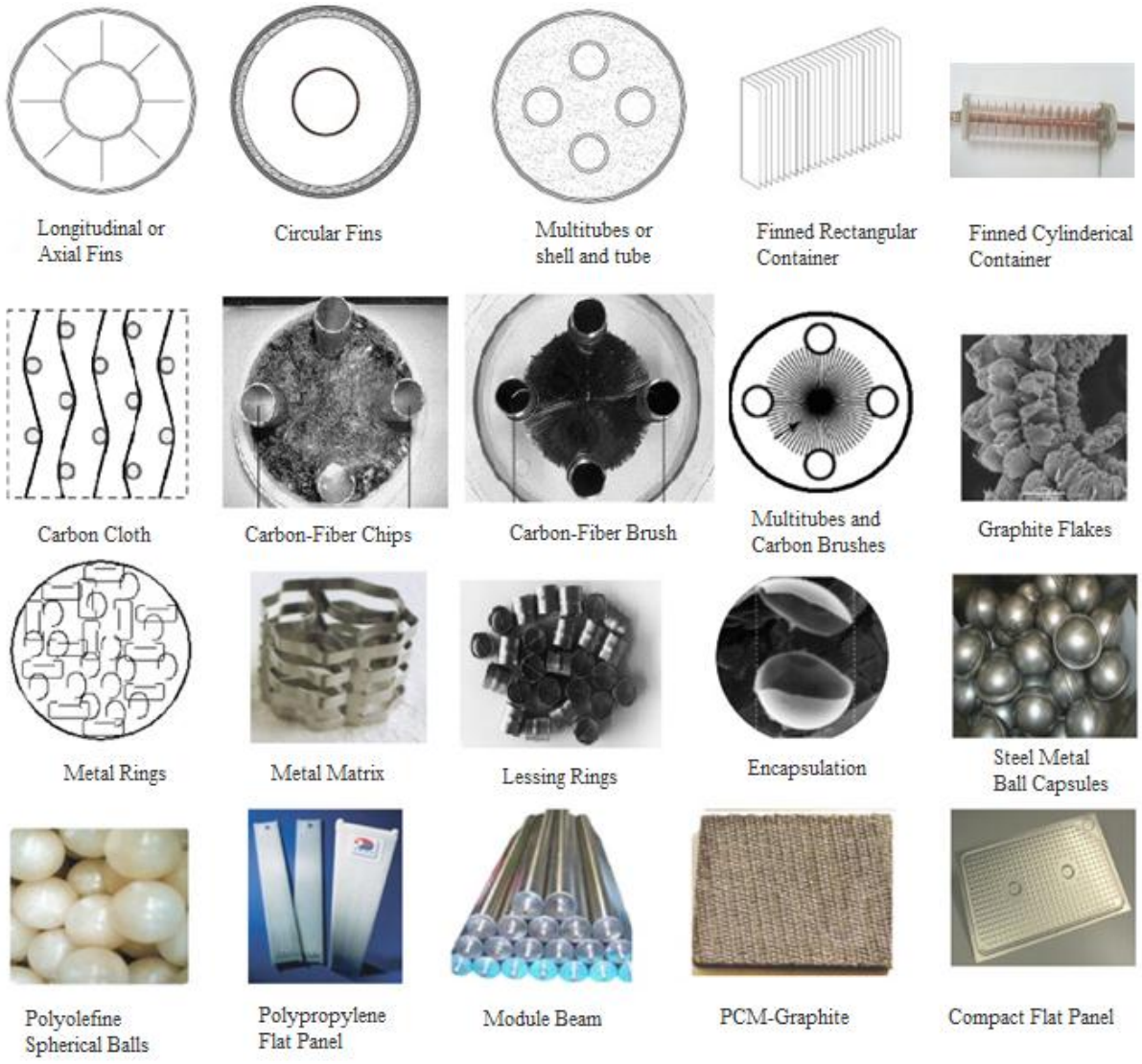

Fig.21. Various techniques used for enhancing thermal performance of LHS system. In this figure, the various techniques adopted by researchers are sequenced on the basis of subchapters of this review paper such as initially various configurations of fins are presented and it is followed by PCM additives to enhance thermal conductivity and lastly the PCM encapsulation techniques.

5. Conclusion

This review paper presents a detail literature survey focused on PCMs categorization, long term stability of PCMs and compatibility with container materials, thermal performance analysis and thermal performance enhancement techniques. Literature survey encouraged to draw the below given conclusions:

- For long term thermal performance of LHS system, the PCM needs to ensure thermal stability, chemical stability and corrosion resistance with container material upon subjecting to extended amount of repeated

thermal cycles. After repeated cycles, the thermo-physical properties of PCM shall not change significantly. It can be deducted from the review that paraffins yield better thermal and chemical stability than salt hydrates after repeated thermal cycles. Salt hydrates faces phase segregation and supercooling, which can be controlled by adding suitable thickener and nucleating agents. $CaCl_2.6H_2O$ is found as the most studied salt hydrate. Before using industrial grade PCMs, it is advised to run the repeated thermal cycle test to check the stability of thermo-physical properties.

- It is noticed that conduction heat transfer and natural convection are responsible for melting behaviour of PCMs in containers with different shapes. In early stages, conduction heat transfer is dominant and as the PCM melts down, natural convection dominates the melting of PCM. Container orientation and geometric parameters have great influence on the melting behaviour of PCMs, such as aspect ratio of rectangular and cylindrical containers, spherical capsules radius and annular cavity eccentricity. Thus, it is important to make sure that the geometric configuration is suitable for certain PCM.
- An enhanced storage performance and phase transition rate can be achieved by using fins in LHS system. The size and number of fins are vital in improving thermal performance of LHS system. It is noticed that inclusion of fins has more impact on improving solidification rate than melting rate. The size and number of fins should be optimized as inclusion of fins reduces storage volume for PCM in container and thus the thermal storage capacity is also affected.
- The melting and solidification rate of PCM can be enhanced significantly by incorporating high thermal conductivity additives as it will increase the thermal conductivity of LHS system. However, the inclusion of high density additives can reduce storage volume for PCM in container and it can lead to loss in storage capacity. Therefore, an optimized amount of additives can only be added to enhance thermal performance.
- Utilization of multi-PCM can produce an increased thermal storage performance of LHS system. It is useful in storing thermal energy at constant temperature difference. Multiple PCMs method yields constant heat flux to the PCM in melting process and to the HTF in solidification process. Most of the studies have been carried out on combination of arbitrary PCMs, thus there is a need of experimental investigation of various combinations of actual PCMs.
- Thermal and mechanical stability is dependent on core-to-coating ratio of encapsulated PCM. Increased ratio will produce weak shell and lower ratio will result in less amount of PCM in encapsulation. Optimization of core-to-coating ratio is required. Similarly, encapsulate material shall possess high

thermal conductivity. Metallic encapsulates like copper, aluminium and steel can be good options but it is challenging to manufacture. Salt hydrates for their high thermal conductivity, diffusion values and mechanical strength can be a good choice as encapsulate materials for organic PCMs. Encapsulation having higher thermal conductivity, lower temperature at external surface and smaller diameter of capsule can increase solidification rate of LHS system.

Acknowledgment

The corresponding author's PhD is match funded by Bournemouth University, UK and National University of Science and Technology (NUST), Pakistan. The author would like to extend sincere gratitude to both parties.

References

[1] D. Morrison, S. Abdel-Khalik. Effects of phase-change energy storage on the performance of air-based and liquid-based solar heating systems. Solar Energy. 20 (1978) 57-67.

[2] A. Ghoneim. Comparison of theoretical models of phase-change and sensible heat storage for air and water-based solar heating systems. Solar Energy. 42 (1989) 209-20.

[3] J. Giro-Paloma, M. Martínez, L.F. Cabeza, A.I. Fernández. Types, methods, techniques, and applications for microencapsulated phase change materials (MPCM): A review. Renewable and Sustainable Energy Reviews. 53 (2016) 1059-75.

[4] R. Jacob, F. Bruno. Review on shell materials used in the encapsulation of phase change materials for high temperature thermal energy storage. Renewable and Sustainable Energy Reviews. 48 (2015) 79-87.

[5] M. Kenisarin, K. Mahkamov. Passive thermal control in residential buildings using phase change materials. Renewable and Sustainable Energy Reviews. 55 (2016) 371-98.

[6] B. Tang, L. Wang, Y. Xu, J. Xiu, S. Zhang. Hexadecanol/phase change polyurethane composite as form-stable phase change material for thermal energy storage. Solar Energy Materials and Solar Cells. 144 (2016) 1-6.

[7] B. Tang, Y. Wang, M. Qiu, S. Zhang. A full-band sunlight-driven carbon nanotube/PEG/SiO 2 composites for solar energy storage. Solar Energy Materials and Solar Cells. 123 (2014) 7-12.

[8] Y. Wang, B. Tang, S. Zhang. Single-Walled Carbon Nanotube/Phase Change Material Composites: Sunlight-Driven, Reversible, Form-Stable Phase Transitions for Solar Thermal Energy Storage. Advanced Functional Materials. 23 (2013) 4354-60.

[9] M. Liu, Y. Ma, H. Wu, R.Y. Wang. Metal Matrix–Metal Nanoparticle Composites with Tunable Melting Temperature and High Thermal Conductivity for Phase-Change Thermal Storage. ACS nano. 9 (2015) 1341-51.

[10] A. Abhat. Low temperature latent heat thermal energy storage: heat storage materials. Solar energy. 30 (1983) 313-32.

[11] A. Sharma, V. Tyagi, C. Chen, D. Buddhi. Review on thermal energy storage with phase change materials and applications. Renewable and Sustainable energy reviews. 13 (2009) 318-45.

[12] B. Zalba, J.M. Marín, L.F. Cabeza, H. Mehling. Review on thermal energy storage with phase change: materials, heat transfer analysis and applications. Applied thermal engineering. 23 (2003) 251-83.

[13] L.F. Cabeza, A. Castell, C. Barreneche, A. De Gracia, A. Fernández. Materials used as PCM in thermal energy storage in buildings: a review. Renewable and Sustainable Energy Reviews. 15 (2011) 1675-95.

[14] M.K. Rathod, J. Banerjee. Thermal stability of phase change materials used in latent heat energy storage systems: a review. Renewable and Sustainable Energy Reviews. 18 (2013) 246-58.

[15] M. Kenisarin, K. Mahkamov. Solar energy storage using phase change materials. Renewable and Sustainable Energy Reviews. 11 (2007) 1913-65.

[16] A.M. Khudhair, M.M. Farid. A review on energy conservation in building applications with thermal storage by latent heat using phase change materials. Energy conversion and management. 45 (2004) 263-75.

[17] M.M. Farid, A.M. Khudhair, S.A.K. Razack, S. Al-Hallaj. A review on phase change energy storage: materials and applications. Energy conversion and management. 45 (2004) 1597-615.

[18] Rubitherm® Technologies GmbH, http://www.rubitherm.eu/en/. 2015.

[19] A. Sari, R. Eroglu, A. Bicer, A. Karaipekli. Synthesis and thermal energy storage properties of erythritol tetrastearate and erythritol tetrapalmitate. Chemical Engineering & Technology. 34 (2011) 87-92.

[20] H. Mehling, L.F. Cabeza. Heat and cold storage with PCM. Springer2008.

[21] M. Esen, A. Durmuş, A. Durmuş. Geometric design of solar-aided latent heat store depending on various parameters and phase change materials. Solar Energy. 62 (1998) 19-28.

[22] H.A. Adine, H. El Qarnia. Numerical analysis of the thermal behaviour of a shell-and-tube heat storage unit using phase change materials. Applied mathematical modelling. 33 (2009) 2132-44.

[23] M. Lacroix. Numerical simulation of a shell-and-tube latent heat thermal energy storage unit. Solar energy. 50 (1993) 357-67.

[24] M. Huang, P. Eames, B. Norton. Thermal regulation of building-integrated photovoltaics using phase change materials. International Journal of Heat and Mass Transfer. 47 (2004) 2715-33.

[25] C. Alkan, K. Kaya, A. Sarı. Preparation, thermal properties and thermal reliability of form-stable paraffin/polypropylene composite for thermal energy storage. Journal of Polymers and the Environment. 17 (2009) 254-8.

[26] M. Hadjieva, J. Argirov. Thermophysical properties of some paraffins applicable to thermal energy storage. Solar Energy Materials and Solar Cells. 27 (1992) 181-7.

[27] A. Sharma, S. Sharma, D. Buddhi. Accelerated thermal cycle test of acetamide, stearic acid and paraffin wax for solar thermal latent heat storage applications. Energy Conversion and Management. 43 (2002) 1923-30.

[28] A. Shukla, D. Buddhi, R. Sawhney. Thermal cycling test of few selected inorganic and organic phase change materials. Renewable Energy. 33 (2008) 2606-14.

[29] H. Mehling, L.F. Cabeza. Phase change materials and their basic properties. Thermal energy storage for sustainable energy consumption. Springer2007. pp. 257-77.

[30] H. Kimura, J. Kai. Feasibility of trichlorofluoromethane (CCl 3 F, R11) heptadecahydrate as a heat storage material. Energy conversion and management. 25 (1985) 179-86.

[31] F.C. Porisini. Salt hydrates used for latent heat storage: corrosion of metals and reliability of thermal performance. Solar Energy. 41 (1988) 193-7.

[32] V.V. Tyagi, D. Buddhi. PCM thermal storage in buildings: a state of art. Renewable and Sustainable Energy Reviews. 11 (2007) 1146-66.

[33] H. Kimura, J. Kai. Phase change stability of CaCl 2· 6H 2 O. Solar Energy. 33 (1984) 557-63.

[34] V. Tyagi, D. Buddhi. Thermal cycle testing of calcium chloride hexahydrate as a possible PCM for latent heat storage. Solar Energy Materials and Solar Cells. 92 (2008) 891-9.

[35] H. Feilchenfeld, S. Sarig. Calcium chloride hexahydrate: A phase-changing material for energy storage. Industrial & engineering chemistry product research and development. 24 (1985) 130-3.

[36] S. Marks. An investigation of the thermal energy storage capacity of Glauber's salt with respect to thermal cycling. Solar Energy. 25 (1980) 255-8.

[37] I. Dincer, M. Rosen. Thermal energy storage: systems and applications. John Wiley & Sons2002.

[38] T. Wada, R. Yamamoto, Y. Matsuo. Heat storage capacity of sodium acetate trihydrate during thermal cycling. Solar Energy. 33 (1984) 373-5.

[39] H. Kimura, J. Kai. Phase change stability of sodium acetate trihydrate and its mixtures. Solar energy. 35 (1985) 527-34.

[40] A. El-Sebaii, S. Al-Amir, F. Al-Marzouki, A.S. Faidah, A. Al-Ghamdi, S. Al-Heniti. Fast thermal cycling of acetanilide and magnesium chloride hexahydrate for indoor solar cooking. Energy conversion and Management. 50 (2009) 3104-11.

[41] A. El-Sebaii, S. Al-Heniti, F. Al-Agel, A. Al-Ghamdi, F. Al-Marzouki. One thousand thermal cycles of magnesium chloride hexahydrate as a promising PCM for indoor solar cooking. Energy Conversion and Management. 52 (2011) 1771-7.

[42] S. Sharma, D. Buddhi, R. Sawhney. Accelerated thermal cycle test of latent heat-storage materials. Solar Energy. 66 (1999) 483-90.

[43] A. Lázaro, B. Zalba, M. Bobi, C. Castellón, L.F. Cabeza. Experimental study on phase change materials and plastics compatibility. AIChE journal. 52 (2006) 804-8.

[44] L. Cabeza, J. Illa, J. Roca, F. Badia, H. Mehling, S. Hiebler, et al. Immersion corrosion tests on metal-salt hydrate pairs used for latent heat storage in the 32 to 36° C temperature range. Materials and Corrosion. 52 (2001) 140-6.

[45] L. Cabeza, J. Illa, J. Roca, F. Badia, H. Mehling, S. Hiebler, et al. Middle term immersion corrosion tests on metal-salt hydrate pairs used for latent heat storage in the 32 to 36° C temperature range. Materials and Corrosion. 52 (2001) 748-54.

[46] L. Cabeza, J. Roca, M. Nogués, H. Mehling, S. Hiebler. Immersion corrosion tests on metal-salt hydrate pairs used for latent heat storage in the 48 to 58° C temperature range. Materials and Corrosion. 53 (2002) 902-7.

[47] A.J. Farrell, B. Norton, D.M. Kennedy. Corrosive effects of salt hydrate phase change materials used with aluminium and copper. Journal of materials processing technology. 175 (2006) 198-205.

[48] K. Nagano, K. Ogawa, T. Mochida, K. Hayashi, H. Ogoshi. Performance of heat charge/discharge of magnesium nitrate hexahydrate and magnesium chloride hexahydrate mixture to a single vertical tube for a latent heat storage system. Applied thermal engineering. 24 (2004) 209-20.

[49] A. García-Romero, A. Delgado, A. Urresti, K. Martín, J. Sala. Corrosion behaviour of several aluminium alloys in contact with a thermal storage phase change material based on Glauber's salt. Corrosion Science. 51 (2009) 1263-72.

[50] P. Moreno, L. Miró, A. Solé, C. Barreneche, C. Solé, I. Martorell, et al. Corrosion of metal and metal alloy containers in contact with phase change materials (PCM) for potential heating and cooling applications. Applied Energy. 125 (2014) 238-45.

[51] F. Agyenim, N. Hewitt, P. Eames, M. Smyth. A review of materials, heat transfer and phase change problem formulation for latent heat thermal energy storage systems (LHTESS). Renewable and Sustainable Energy Reviews. 14 (2010) 615-28.

[52] M. Liu, W. Saman, F. Bruno. Review on storage materials and thermal performance enhancement techniques for high temperature phase change thermal storage systems. Renewable and Sustainable Energy Reviews. 16 (2012) 2118-32.

[53] J. Khodadadi, L. Fan, H. Babaei. Thermal conductivity enhancement of nanostructure-based colloidal suspensions utilized as phase change materials for thermal energy storage: a review. Renewable and Sustainable Energy Reviews. 24 (2013) 418-44.

[54] P. Lamberg, R. Lehtiniemi, A.-M. Henell. Numerical and experimental investigation of melting and freezing processes in phase change material storage. International Journal of Thermal Sciences. 43 (2004) 277-87.

[55] B. Kamkari, H. Shokouhmand, F. Bruno. Experimental investigation of the effect of inclination angle on convection-driven melting of phase change material in a rectangular enclosure. International Journal of Heat and Mass Transfer. 72 (2014) 186-200.

[56] F. Tan. Constrained and unconstrained melting inside a sphere. International Communications in Heat and Mass Transfer. 35 (2008) 466-75.

[57] B.J. Jones, D. Sun, S. Krishnan, S.V. Garimella. Experimental and numerical study of melting in a cylinder. International Journal of Heat and Mass Transfer. 49 (2006) 2724-38.

[58] H. Shmueli, G. Ziskind, R. Letan. Melting in a vertical cylindrical tube: numerical investigation and comparison with experiments. International Journal of Heat and Mass Transfer. 53 (2010) 4082-91.

[59] M. Esapour, M. Hosseini, A. Ranjbar, Y. Pahamli, R. Bahrampoury. Phase change in multi-tube heat exchangers. Renewable Energy. 85 (2016) 1017-25.

[60] N. Vyshak, G. Jilani. Numerical analysis of latent heat thermal energy storage system. Energy Conversion and Management. 48 (2007) 2161-8.

[61] B. Zivkovic, I. Fujii. An analysis of isothermal phase change of phase change material within rectangular and cylindrical containers. Solar Energy. 70 (2001) 51-61.

[62] S. Seddegh, X. Wang, A.D. Henderson. A comparative study of thermal behaviour of a horizontal and vertical shell-and-tube energy storage using phase change materials. Applied Thermal Engineering. 93 (2016) 348-58.

[63] M.J. Allen, N. Sharifi, A. Faghri, T.L. Bergman. Effect of inclination angle during melting and solidification of a phase change material using a combined heat pipe-metal foam or foil configuration. International Journal of Heat and Mass Transfer. 80 (2015) 767-80.

[64] R. Akhilesh, A. Narasimhan, C. Balaji. Method to improve geometry for heat transfer enhancement in PCM composite heat sinks. International Journal of Heat and Mass Transfer. 48 (2005) 2759-70.

[65] M. Gharebaghi, I. Sezai. Enhancement of heat transfer in latent heat storage modules with internal fins. Numerical Heat Transfer, Part A: Applications. 53 (2007) 749-65.

[66] M. Lacroix, M. Benmadda. Numerical simulation of natural convection-dominated melting and solidification from a finned vertical wall. Numerical Heat Transfer, Part A Applications. 31 (1997) 71-86.

[67] V. Shatikian, G. Ziskind, R. Letan. Numerical investigation of a PCM-based heat sink with internal fins. International Journal of Heat and Mass Transfer. 48 (2005) 3689-706.

[68] U. Stritih. An experimental study of enhanced heat transfer in rectangular PCM thermal storage. International Journal of Heat and Mass Transfer. 47 (2004) 2841-7.

[69] Y. Tao, Y. He. Effects of natural convection on latent heat storage performance of salt in a horizontal concentric tube. Applied Energy. 143 (2015) 38-46.

[70] C. Guo, W. Zhang. Numerical simulation and parametric study on new type of high temperature latent heat thermal energy storage system. Energy Conversion and Management. 49 (2008) 919-27.

[71] M. Lacroix. Study of the heat transfer behavior of a latent heat thermal energy storage unit with a finned tube. International Journal of Heat and Mass Transfer. 36 (1993) 2083-92.

[72] Y. Zhang, A. Faghri. Heat transfer enhancement in latent heat thermal energy storage system by using an external radial finned tube. Journal of Enhanced Heat Transfer. 3 (1996).

[73] M. Rahimi, A. Ranjbar, D. Ganji, K. Sedighi, M. Hosseini, R. Bahrampoury. Analysis of geometrical and operational parameters of PCM in a fin and tube heat exchanger. International Communications in Heat and Mass Transfer. 53 (2014) 109-15.

[74] J.C. Choi, S.D. Kim. Heat-transfer characteristics of a latent heat storage system using MgCl 2· 6H 2 O. Energy. 17 (1992) 1153-64.

[75] R. Velraj, R. Seeniraj, B. Hafner, C. Faber, K. Schwarzer. Experimental analysis and numerical modelling of inward solidification on a finned vertical tube for a latent heat storage unit. Solar Energy. 60 (1997) 281-90.

[76] M.K. Rathod, J. Banerjee. Thermal performance enhancement of shell and tube Latent Heat Storage Unit using longitudinal fins. Applied Thermal Engineering. 75 (2015) 1084-92.

[77] F. Agyenim, P. Eames, M. Smyth. A comparison of heat transfer enhancement in a medium temperature thermal energy storage heat exchanger using fins. Solar Energy. 83 (2009) 1509-20.

[78] M. Medrano, M. Yilmaz, M. Nogués, I. Martorell, J. Roca, L.F. Cabeza. Experimental evaluation of commercial heat exchangers for use as PCM thermal storage systems. Applied Energy. 86 (2009) 2047-55.

[79] D. Chung. A review of exfoliated graphite. Journal of Materials Science. 51 (2016) 554-68.

[80] L. Fan, J. Khodadadi. Thermal conductivity enhancement of phase change materials for thermal energy storage: a review. Renewable and Sustainable Energy Reviews. 15 (2011) 24-46.

[81] T. Fiedler, A. Öchsner, I.V. Belova, G.E. Murch. Thermal conductivity enhancement of compact heat sinks using cellular metals. Defect and Diffusion Forum. Trans Tech Publ2008. pp. 222-6.

[82] O. Mesalhy, K. Lafdi, A. Elgafy, K. Bowman. Numerical study for enhancing the thermal conductivity of phase change material (PCM) storage using high thermal conductivity porous matrix. Energy Conversion and Management. 46 (2005) 847-67.

[83] D. Haillot, X. Py, V. Goetz, M. Benabdelkarim. Storage composites for the optimisation of solar water heating systems. Chemical engineering research and design. 86 (2008) 612-7.

[84] A. Sarı, A. Karaipekli. Thermal conductivity and latent heat thermal energy storage characteristics of paraffin/expanded graphite composite as phase change material. Applied Thermal Engineering. 27 (2007) 1271-7.

[85] Z.-j. Duan, H.-z. Zhang, L.-x. Sun, Z. Cao, F. Xu, Y.-j. Zou, et al. CaCl2· 6H2O/Expanded graphite composite as form-stable phase change materials for thermal energy storage. Journal of Thermal Analysis and Calorimetry. 115 (2014) 111-7.

[86] Y. Wu, T. Wang. Hydrated salts/expanded graphite composite with high thermal conductivity as a shape-stabilized phase change material for thermal energy storage. Energy Conversion and Management. 101 (2015) 164-71.

[87] H.K. Shin, M. Park, H.-Y. Kim, S.-J. Park. Thermal property and latent heat energy storage behavior of sodium acetate trihydrate composites containing expanded graphite and carboxymethyl cellulose for phase change materials. Applied Thermal Engineering. 75 (2015) 978-83.

[88] M. Dannemand, J.B. Johansen, S. Furbo. Solidification behavior and thermal conductivity of bulk sodium acetate trihydrate composites with thickening agents and graphite. Solar Energy Materials and Solar Cells. 145 (2016) 287-95.

[89] E.-B.S. Mettawee, G.M. Assassa. Thermal conductivity enhancement in a latent heat storage system. Solar Energy. 81 (2007) 839-45.

[90] J. Zeng, L. Sun, F. Xu, Z. Tan, Z. Zhang, J. Zhang, et al. Study of a PCM based energy storage system containing Ag nanoparticles. Journal of Thermal Analysis and Calorimetry. 87 (2006) 371-5.

[91] R. Velraj, R. Seeniraj, B. Hafner, C. Faber, K. Schwarzer. Heat transfer enhancement in a latent heat storage system. Solar energy. 65 (1999) 171-80.

[92] A. Elgafy, K. Lafdi. Effect of carbon nanofiber additives on thermal behavior of phase change materials. Carbon. 43 (2005) 3067-74.

[93] J. Fukai, M. Kanou, Y. Kodama, O. Miyatake. Thermal conductivity enhancement of energy storage media using carbon fibers. Energy Conversion and Management. 41 (2000) 1543-56.

[94] J. Fukai, Y. Hamada, Y. Morozumi, O. Miyatake. Improvement of thermal characteristics of latent heat thermal energy storage units using carbon-fiber brushes: experiments and modeling. International Journal of Heat and Mass Transfer. 46 (2003) 4513-25.

[95] F. Dinter, M.A. Geyer, R. Tamme. Thermal energy storage for commercial applications: a feasibility study on economic storage systems. Springer1991.

[96] J. Wang, G. Chen, H. Jiang. Theoretical study on a novel phase change process. International journal of energy research. 23 (1999) 287-94.

[97] A. Mosaffa, C.I. Ferreira, F. Talati, M. Rosen. Thermal performance of a multiple PCM thermal storage unit for free cooling. Energy Conversion and Management. 67 (2013) 1-7.

[98] Z.-X. Gong, A.S. Mujumdar. Enhancement of energy charge-discharge rates in composite slabs of different phase change materials. International Journal of Heat and Mass Transfer. 39 (1996) 725-33.

[99] M.M. Farid, A. Kanzawa. Thermal performance of a heat storage module using PCM's with different melting temperatures: mathematical modeling. Journal of solar energy engineering. 111 (1989) 152-7.

[100] M.M. Farid, Y. Kim, A. Kansawa. Thermal performance of a heat storage module using PCM's with different melting temperature: experimental. Journal of Solar Energy Engineering. 112 (1990) 125-31.

[101] T.K. Aldoss, M.M. Rahman. Comparison between the single-PCM and multi-PCM thermal energy storage design. Energy Conversion and Management. 83 (2014) 79-87.

[102] J. Wang, Y. Ouyang, G. Chen. Experimental study on charging processes of a cylindrical heat storage capsule employing multiple-phase-change materials. International journal of energy research. 25 (2001) 439-47.

[103] C. Liu, Z. Rao, J. Zhao, Y. Huo, Y. Li. Review on nanoencapsulated phase change materials: Preparation, characterization and heat transfer enhancement. Nano Energy. (2015).

[104] T. Khadiran, M.Z. Hussein, Z. Zainal, R. Rusli. Encapsulation techniques for organic phase change materials as thermal energy storage medium: A review. Solar Energy Materials and Solar Cells. 143 (2015) 78-98.

[105] M. Delgado, A. Lázaro, J. Mazo, B. Zalba. Review on phase change material emulsions and microencapsulated phase change material slurries: materials, heat transfer studies and applications. Renewable and Sustainable Energy Reviews. 16 (2012) 253-73.

[106] A. Jamekhorshid, S. Sadrameli, M. Farid. A review of microencapsulation methods of phase change materials (PCMs) as a thermal energy storage (TES) medium. Renewable and Sustainable Energy Reviews. 31 (2014) 531-42.

[107] C.-Y. Zhao, G.H. Zhang. Review on microencapsulated phase change materials (MEPCMs): fabrication, characterization and applications. Renewable and Sustainable Energy Reviews. 15 (2011) 3813-32.

[108] L.F. Cabeza. Advances in Thermal Energy Storage Systems: Methods and Applications. Elsevier Science & Technology2014.

[109] T. Ohtsubo, S. Tsuda, K. Tsuji. A study of the physical strength of fenitrothion microcapsules. Polymer. 32 (1991) 2395-9.

[110] H. Zhang, X. Wang. Synthesis and properties of microencapsulated n-octadecane with polyurea shells containing different soft segments for heat energy storage and thermal regulation. Solar Energy Materials and Solar Cells. 93 (2009) 1366-76.

[111] S. Namwong, M.Z. Islam, S. Noppalit, P. Tangboriboonrat, P. Chaiyasat, A. Chaiyasat. Encapsulation of octadecane in poly (divinylbenzene-co-methyl methacrylate) using phase inversion emulsification for droplet generation. Journal of Macromolecular Science, Part A. 53 (2016) 11-7.

[112] S. Yu, X. Wang, D. Wu. Microencapsulation of n-octadecane phase change material with calcium carbonate shell for enhancement of thermal conductivity and serving durability: synthesis, microstructure, and performance evaluation. Applied Energy. 114 (2014) 632-43.

[113] Y. Yang, X. Ye, J. Luo, G. Song, Y. Liu, G. Tang. Polymethyl methacrylate based phase change microencapsulation for solar energy storage with silicon nitride. Solar Energy. 115 (2015) 289-96.

[114] N. SARIER, E. ONDER, G. UKUSER. Silver Incorporated Microencapsulation of n-Hexadecane and n-Octadecane Appropriate for Dynamic Thermal Management in Textiles. Thermochimica Acta. (2015).

[115] X. Jiang, R. Luo, F. Peng, Y. Fang, T. Akiyama, S. Wang. Synthesis, characterization and thermal properties of paraffin microcapsules modified with nano-Al 2 O 3. Applied Energy. 137 (2015) 731-7.

[116] C. Alkan, A. Sarı, A. Karaipekli, O. Uzun. Preparation, characterization, and thermal properties of microencapsulated phase change material for thermal energy storage. Solar Energy Materials and Solar Cells. 93 (2009) 143-7.

[117] S. Ma, G. Song, W. Li, P. Fan, G. Tang. UV irradiation-initiated MMA polymerization to prepare microcapsules containing phase change paraffin. Solar Energy Materials and Solar Cells. 94 (2010) 1643-7.

[118] M. Hawlader, M. Uddin, H. Zhu. Encapsulated phase change materials for thermal energy storage: experiments and simulation. International Journal of Energy Research. 26 (2002) 159-71.

[119] T.E. Alam, J.S. Dhau, D.Y. Goswami, E. Stefanakos. Macroencapsulation and characterization of phase change materials for latent heat thermal energy storage systems. Applied Energy. 154 (2015) 92-101.

[120] L.F. Cabeza, M. Ibanez, C. Sole, J. Roca, M. Nogués. Experimentation with a water tank including a PCM module. Solar Energy Materials and Solar Cells. 90 (2006) 1273-82.

[121] H. Mehling, L.F. Cabeza, S. Hippeli, S. Hiebler. PCM-module to improve hot water heat stores with stratification. Renewable energy. 28 (2003) 699-711.

[122] M. Veerappan, S. Kalaiselvam, S. Iniyan, R. Goic. Phase change characteristic study of spherical PCMs in solar energy storage. Solar Energy. 83 (2009) 1245-52.

[123] N. Calvet, X. Py, R. Olivès, J.-P. Bédécarrats, J.-P. Dumas, F. Jay. Enhanced performances of macro-encapsulated phase change materials (PCMs) by intensification of the internal effective thermal conductivity. Energy. 55 (2013) 956-64.

[124] H. Zhang, J. Baeyens, J. Degrève, G. Cáceres, R. Segal, F. Pitié. Latent heat storage with tubular-encapsulated phase change materials (PCMs). Energy. 76 (2014) 66-72.

[125] J. Wei, Y. Kawaguchi, S. Hirano, H. Takeuchi. Study on a PCM heat storage system for rapid heat supply. Applied thermal engineering. 25 (2005) 2903-20.

[126] K. Ismail, J. Henrıquez. Solidification of PCM inside a spherical capsule. Energy conversion and management. 41 (2000) 173-87.

[127] K. Ismail, R. Moraes. A numerical and experimental investigation of different containers and PCM options for cold storage modular units for domestic applications. International Journal of Heat and Mass Transfer. 52 (2009) 4195-202.